UNIVERSITÄT KARLSRUHE

Nonlinear solution methods for infinitesimal perfect plasticity

Christian Wieners

Preprint Nr. 06/11

Institut für Wissenschaftliches Rechnen
und Mathematische Modellbildung

76128 Karlsruhe

Anschrift des Verfassers:

Prof. Dr. Christian Wieners
Institut für Angewandte und Numerische Mathematik
Universität Karlsruhe
D-76128 Karlsruhe

Nonlinear solution methods for infinitesimal perfect plasticity

Christian Wieners

Abstract. We review the classical return algorithm for incremental plasticity in the context of nonlinear programming, and we discuss the algorithmic realization of the SQP method for infinitesimal perfect plasticity. We show that the radial return corresponds to an orthogonal projection onto the convex set of admissible stresses. Inserting this projection into the equilibrium equation results in a semismooth equation which can be solved by a generalized Newton method. Alternatively, an appropriate linearization of the projection is equivalent to the SQP method, which is shown to be more robust as the classical radial return. This is illustrated by a numerical comparison of both methods for a benchmark problem.

1. Introduction

Concepts of *convex analysis* play an important role in the mathematical research of infinitesimal plasticity, and fundamental results have been obtained (see, e. g., Temam [**15**]). On the other hand, concepts of *convex programming* for discretized plasticity have not been considered systematically (only a few results are available, e. g., by Carstensen et al. [**1**] and Christensen [**3**]).

The purpose of this paper is to provide a better understanding of known algorithms, the development of new algorithms for incremental plasticity, and the presentation of the algorithms in a unified framework by the consequent application of convex programming techniques.

The incremental problem in infinitesimal plasticity is commonly solved by the closest projection method (radial return), see, e. g., [**13**]. It was already observed in [**1**] that this algorithm corresponds to a convex minimization problem for the displacements. Since in the general case, the primal displacement solution is not unique, this minimization problem cannot be strictly convex. Moreover, since the discrete primal solution in perfect plasticity is mesh-dependent and robust estimates are available only in measure valued spaces, we cannot expect mesh-independent convergence.

By duality, incremental plasticity can be reformulated as a constraint convex minimization problem for the stresses which can be solved, e. g., by SQP methods. Since the dual problem is uniformly convex, we may expect robust convergence.

Algorithmically, the main idea can be illustrated geometrically (cf. Figure 1 and Figure 2). The incremental problem in plasticity solves three equations: the *flow rule* for the increment of the plastic strain, the *complementarity conditions* for flow function and plastic multiplier, and the *equilibrium equation* for the stress. The radial return (corresponding to an *orthogonal projection*) solves the flow rule and the complementarity conditions independently for every material point, and this (nonlinear) material response is inserted into the equilibrium equation. The SQP method (corresponding to an *projection onto a half space* containing the convex set of admissible stresses) solves in every step only a linearized flow rule and linearized complementarity conditions, and this linearized material response is inserted into the

1991 *Mathematics Subject Classification.* 65N55, 65F10.
Key words and phrases. Plasticity, Radial Return, SQP Methods.

equilibrium equation. We show that this simplification (replacing the full nonlinear material response with the linearization) leads to a substantial gain of efficiency.

The paper is organized as follows. Since the construction of SQP methods is quite technical, we describe this method first in a general setting (Table 1), then for orthogonal projections (Table 2), and finally for incremental plasticity (Table 3). We start in Section 2 with a review on nonsmooth methods, recalling generalized Newton methods for Lipschitz functions and SQP methods for constraint convex minimization problems in an abstract framework. Next, we recall the well-known closest point projection onto the convex set of admissible stresses, and we propose a SQP method for the evaluation of the projection. Then, we explain the main idea for static plasticity in Section 4, before we consider the incremental problem in infinitesimal plasticity in Section 5. There, we consider its dual formulation, and an existence result is proved for the incremental solution (provided that a suitable Slater condition is satisfied).

The main result is presented in Section 7 where we derive the classical projection method and develop the new SQP method. Both algorithms are compared explicitly by a detailed description of the algorithmic realization. They were implemented for the special case of von Mises plasticity, and a numerical evaluation for a standard benchmark problem is finally given.

For simplicity, we restrict ourselves to the classical Prandtl-Reuss model in infinitesimal perfect plasticity where plasticity is determined by a (possibly multi-dimensional) yield surface and an associated flow rule. Moreover, we restrict ourselves to the discrete problem. The dependence on discretization parameters is studied only experimentally (see Table 6). The analysis of these methods with respect to mesh-independence is beyond the scope of this work; this would require the investigation of the proposed algorithms in function spaces as it is done for control problems, e. g., by Hintermüller et. al. [**6, 7**].

2. Nonsmooth methods

We shortly review two classes of well established methods in nonlinear programming: a generalized Newton method for nonsmooth functions, and the SQP method for constraint problems. For more details on these methods see, e. g., [**4, 10**].

Generalized Newton methods. Let X be a finite dimensional space and $f\colon X \longrightarrow X$ be a Lipschitz continuous function. Then, f is almost everywhere differentiable, and for $x, v \in X$ the directional derivatives

$$Df(x;v) = \limsup_{t\downarrow 0, y\to x} \frac{1}{t}\Big(f(y+tv) - f(y)\Big)$$

exist. The convex hull $\partial f(x) = \operatorname{conv}\{Df(x;v)\colon v \in X\}$ builds the generalized Jacobian as it is introduced by Clarke (see, e. g., [**8**] for the definition and for properties of generalized derivatives). The corresponding generalized Newton method for the equation $f(x) = 0$ reads as follows: starting with $x^0 \in X$, find Δx^k such that

$$0 \in f(x^{k-1}) + \partial f(x^{k-1})\Delta x^k, \qquad k = 1, 2, 3, ...$$

and set $x^k = x^{k-1} + \Delta x^k$. A realization of this method requires a choice $C_k \in \partial f(x^{k-1})$ such that the linear problem $C_k \Delta x^k = -f(x^{k-1})$ has a solution (see, e. g., [**8**] for the analysis of generalized Newton methods for Lipschitz equations).

Convex minimization. For the special case that $f = DF$ is the derivative of a convex potential $F\colon X \longrightarrow \mathbf{R}$, any minimizer $x \in X$ of $F(\cdot)$ solves the equation $f(x) = 0$, and a suitably damped Newton iteration generates a monotonically nonincreasing sequence of $F(\cdot)$ since all $C \in \partial f(x)$ are positive semi-definite (see, e. g., [**11**] for global convergence in the uniformly convex case).

Convex constraint minimization. Now, we consider an additional constraint: find a minimizer $x \in X$ of $F(\cdot)$ subject to $g(x) \leq 0$, where $g\colon X \longrightarrow \mathbf{R}$ is a convex smooth function. If the admissible set is not empty, a minimizer of the constraint problem exists. If, in addition, a strictly admissible element $\hat{x} \in X$ with $g(\hat{x}) < 0$ exists, a Lagrange parameter $y \geq 0$ exists such that (x, y) is a critical point of the Lagrange functional $L(x,y) = F(x) + y\, g(x)$, which is characterized by the KKT-system

$$\begin{aligned} &0 = f(x) + yDg(x) \ , \\ &g(x) \leq 0, \quad y \geq 0, \quad y\, g(x) = 0 \ . \end{aligned}$$

The corresponding Lagrange-Newton method considers the Lipschitz continuous problem

$$\begin{aligned} &0 = f(x) + yDg(x) \ , \\ &0 = \max\{0, g(x)\} \ . \end{aligned}$$

A generalized Newton step for this system reads as follows: for given (x^{k-1}, y^{k-1}) find $(\Delta x^k, \Delta y^k)$ such that

$$\begin{aligned} 0 &\in f(x^{k-1}) + y^{k-1}Dg(x^{k-1}) + \partial f(x^{k-1})\Delta x^k + y^{k-1}D^2g(x^{k-1})\Delta x^k + \Delta y^k Dg(x^{k-1}) \ , \\ 0 &\in \max\{0, g(x^{k-1})\} + \partial \max\{0, g(x^{k-1})\}Dg(x^{k-1})\Delta x^k \ , \end{aligned}$$

where

$$\partial \max\{0, g(x^{k-1})\} = \begin{cases} \{0\} & g(x^{k-1}) < 0, \\ \mathrm{conv}\{0, g'(x^{k-1})\} & g(x^{k-1}) = 0, \\ \{g'(x^{k-1})\} & g(x^{k-1}) > 0. \end{cases}$$

The SQP method. Since the Lagrange-Newton method does not necessarily fulfill the complementary conditions $y \geq 0$ and $y\, g(x) = 0$, we use the corresponding SQP method. This is obtained by replacing the generalized Newton iteration by a sequence of quadratic minimization problems with linearized constraints. Therefore, the generalized Newton step for the Lagrange system is modified to

$$0 = f(x^{k-1}) + y^{k-1}Dg(x^{k-1}) + C_k\Delta x^k + y^{k-1}D^2g(x^{k-1})\Delta x^k + \Delta y^k Dg(x^{k-1}) \ , \tag{1a}$$

$$g(x^{k-1}) + Dg(x^{k-1})\Delta x^k \leq 0, \quad y^k \geq 0, \quad y^k\big(g(x^{k-1}) + Dg(x^{k-1})\Delta x^k\big) = 0 \tag{1b}$$

with some $C_k \in \partial f(x^{k-1})$. Introducing the quadratic and linear functionals

$$\begin{aligned} F_k(\Delta x) &= f(x^{k-1}) \cdot \Delta x + \frac{1}{2}\Delta x \cdot \big(C_k + y^{k-1}D^2g(x^{k-1})\big)\Delta x \\ g_k(\Delta x) &= g(x^{k-1}) + Dg(x^{k-1})\Delta x \ , \end{aligned}$$

and using $Dg(x^{k-1}) = Dg_k(\Delta x^k)$, the system (1) has the form

$$\begin{aligned} &0 = DF_k(\Delta x^k) + y^k Dg_k(\Delta x^k) \ , \\ &g_k(\Delta x^k) \leq 0, \quad y^k \geq 0, \quad y^k g_k(\Delta x^k) = 0 \ . \end{aligned}$$

This is the KKT-system of a quadratic program: find a minimizer Δx^k of $F_k(\cdot)$ subject to $g_k(\cdot) \leq 0$. Successively solving (1) for $k = 1, 2, 3, \ldots$ results in the SQP method which is summarized in Table 1. For the application of these methods to plasticity in the following sections, we will specify X, F, f and g.

SQP0)	Start with $x^0 \in X$ and $y^0 \geq 0$. Set $k = 1$.
SQP1)	Find $\Delta x^k \in X$ and $y^k \in \mathbf{R}$ solving $0 = DF_k(\Delta x^k) + y^k Dg_k(x^{k-1})$, $g_k(\Delta x^k) \leq 0,\ y^k \geq 0,\ y^k g_k(\Delta x^k) = 0,$ where $F_k(\Delta x) = f(x^{k-1}) \cdot \Delta x + \frac{1}{2}\Delta x \cdot \big(C_k + y^{k-1}D^2 g(x^{k-1})\big)\Delta x$, $C_k \in \partial f(x^{k-1})$, and $g_k(\Delta x) = g(x^{k-1}) + Dg(x^{k-1})\Delta x$. Set $x^k = x^{k-1} + \Delta x^k$.
SQP3)	If $f(x^k) + y^k Dg(x^k)$ and $\max\{0, g(x^k)\}$ are small enough, stop.
SQP4)	Set $k := k + 1$ and go to SQP1).

Table 1: SQP method for the approximation of a critical point $(x, y) \in X \times \mathbf{R}_{\geq 0}$ of the Lagrange functional $L(x, y) = f(x) + yg(x)$. The algorithm can be extended by a suitable damping strategy which guarantees global convergence in the convex case **[14, 2]**.

3. The closest point projection

Before we study the full equations of plasticity, we discuss the equations for the strain–stress relation independently in every material point. Here, every strain tensor $\boldsymbol{\varepsilon} \in \mathrm{Sym}(d)$ is identified with its linear elastic trial stress $\boldsymbol{\theta} = \mathbb{C} : \boldsymbol{\varepsilon}$. In this paper, we restrict ourselves to material models where the incremental material response depends solely on $\boldsymbol{\theta}$.

Preliminaries. Let $\mathrm{Sym}(d) = \{\boldsymbol{\tau} \in \mathbf{R}^{d,d} \colon \boldsymbol{\tau}^T = \boldsymbol{\tau}\}$ be the set of symmetric matrices. The elastic material properties (in the infinitesimal model) are defined by the Hookian tensor $\mathbb{C}\colon \mathrm{Sym}(d) \longrightarrow \mathrm{Sym}(d)$ defined by $\mathbb{C} : \boldsymbol{\varepsilon} = 2\mu\boldsymbol{\varepsilon} + \lambda\,\mathrm{trace}(\boldsymbol{\varepsilon})\mathbf{I}$, depending on the Lamé constants $\lambda, \mu > 0$. On $\mathrm{Sym}(d)$, the Hookian tensor is positive definite, and the corresponding inner product and the associated energy are denoted by

$$e(\boldsymbol{\sigma}, \boldsymbol{\tau}) = \boldsymbol{\sigma} : \mathbb{C}^{-1} : \boldsymbol{\tau}\ , \qquad E(\boldsymbol{\sigma}) = \frac{1}{2}\, e(\boldsymbol{\sigma}, \boldsymbol{\sigma})\ .$$

The inelastic material behavior is modeled by a convex function

$$\phi\colon \mathrm{Sym}(d) \longrightarrow \mathbf{R}^r$$

determining the convex set of admissible stresses $\mathbf{K} = \{\boldsymbol{\sigma} \in \mathrm{Sym}(d) \colon \phi(\boldsymbol{\sigma}) \leq 0\}$. We assume that ϕ is smooth for $\boldsymbol{\sigma} \neq \mathbf{0}$ and $\phi(\mathbf{0}) < 0$. In the case of single surface plasticity we have $r = 1$, and for $r > 1$, the admissible set $\mathbf{K}$ is the intersection obtained from the convex constraints $\phi_i(\boldsymbol{\sigma}) \leq 0$ for $i = 1, ..., r$.

The convex projection. Let $P_{\mathbf{K}}\colon \mathrm{Sym}(d) \longrightarrow \mathbf{K}$ be the orthogonal projection onto the convex set of admissible stresses with respect to the inner product $e(\cdot, \cdot)$.

LEMMA 1. *For given $\boldsymbol{\theta} \in \mathrm{Sym}(d)$ the projection $\boldsymbol{\sigma} = P_{\mathbf{K}}(\boldsymbol{\theta}) \in \mathbf{K}$ is uniquely determined by the solution $(\boldsymbol{\sigma}, \gamma) \in \mathrm{Sym}(d) \times \mathbf{R}$ of the KKT-system*

$$\mathbf{0} = \boldsymbol{\sigma} - \boldsymbol{\theta} + \gamma \cdot \mathbb{C} : D\phi(\boldsymbol{\sigma})\ , \tag{2a}$$

$$\phi(\boldsymbol{\sigma}) \leq 0, \quad \gamma \cdot \phi(\boldsymbol{\sigma}) = 0, \quad \gamma \geq 0. \tag{2b}$$

PROOF. The projection is characterized by the constraint minimization problem

$$\boldsymbol{\sigma} \in \mathrm{Sym}(d)\colon \qquad E(\boldsymbol{\sigma} - \boldsymbol{\theta}) = \min \qquad \text{subject to } \phi(\boldsymbol{\sigma}) \leq 0\ .$$

Since $E(\cdot)$ is uniformly convex and the problem is strictly admissible (by the assumption $\phi(\mathbf{0}) < 0$), a unique minimizer $\boldsymbol{\sigma}$ and a Lagrange parameter $\gamma \geq 0$ exist such that $(\boldsymbol{\sigma}, \gamma)$ is a saddle point of the Lagrange functional

$$L(\boldsymbol{\sigma}, \gamma) = E(\boldsymbol{\sigma} - \boldsymbol{\theta}) + \gamma \cdot \phi(\boldsymbol{\sigma})$$

which is characterized by the corresponding KKT-system (2). □

The convex potential. The corresponding convex potentials are denoted by

$$\varphi_{\mathbf{K}}(\boldsymbol{\theta}) = E\big(\boldsymbol{\theta} - P_{\mathbf{K}}(\boldsymbol{\theta})\big)\ , \qquad \psi_{\mathbf{K}}(\boldsymbol{\theta}) = E(\boldsymbol{\theta}) - E\big(\boldsymbol{\theta} - P_{\mathbf{K}}(\boldsymbol{\theta})\big), \qquad \boldsymbol{\theta} \in \mathrm{Sym}(d)\,.$$

These potentials will be used in Lemma 5 below to formulate the primal minimization problem. Note that we have by [**5**, Lem. 8.6]

$$D\varphi_{\mathbf{K}}(\boldsymbol{\theta})[\boldsymbol{\eta}] = e\big(\boldsymbol{\theta} - P_{\mathbf{K}}(\boldsymbol{\theta}), \boldsymbol{\eta}\big)\ , \qquad \boldsymbol{\theta}, \boldsymbol{\eta} \in \mathrm{Sym}(d)\ . \tag{3}$$

LEMMA 2. *The functional $\psi_{\mathbf{K}}(\cdot)$ is convex, nonnegative, and we have*

$$D\psi_{\mathbf{K}}(\boldsymbol{\theta})[\boldsymbol{\eta}] = e(P_{\mathbf{K}}(\boldsymbol{\theta}), \boldsymbol{\eta})\ , \qquad \boldsymbol{\theta},\ \boldsymbol{\eta} \in \mathrm{Sym}(d)\ . \tag{4}$$

PROOF. The orthogonal projection $P_{\mathbf{K}}$ is uniquely characterized by

$$e\big(\boldsymbol{\theta} - P_{\mathbf{K}}(\boldsymbol{\theta}), \boldsymbol{\eta} - P_{\mathbf{K}}(\boldsymbol{\theta})\big) \leq 0, \qquad \boldsymbol{\theta} \in \mathrm{Sym}(d),\ \boldsymbol{\eta} \in \mathbf{K}\ . \tag{5}$$

Inserting (3) gives $D\psi_{\mathbf{K}}(\boldsymbol{\theta})[\boldsymbol{\eta}] = e(\boldsymbol{\theta}, \boldsymbol{\eta}) - D\varphi_{\mathbf{K}}(\boldsymbol{\theta})[\boldsymbol{\eta}] = e(P_{\mathbf{K}}(\boldsymbol{\theta}), \boldsymbol{\eta})$, and we obtain from (5) for $\boldsymbol{\theta}, \boldsymbol{\eta} \in \mathrm{Sym}(d)$

$$\begin{aligned}
&\psi_{\mathbf{K}}(\boldsymbol{\theta}) - \psi_{\mathbf{K}}(\boldsymbol{\eta}) - D\psi_{\mathbf{K}}(\boldsymbol{\eta})[\boldsymbol{\theta} - \boldsymbol{\eta}] \\
&\quad = e(P_{\mathbf{K}}(\boldsymbol{\theta}), \boldsymbol{\theta}) - E(P_{\mathbf{K}}(\boldsymbol{\theta})) - e(P_{\mathbf{K}}(\boldsymbol{\eta}), \boldsymbol{\eta}) + E(P_{\mathbf{K}}(\boldsymbol{\eta})) - e(P_{\mathbf{K}}(\boldsymbol{\eta}), \boldsymbol{\theta} - \boldsymbol{\eta}) \\
&\quad = e\big(P_{\mathbf{K}}(\boldsymbol{\theta}) - P_{\mathbf{K}}(\boldsymbol{\eta}), \boldsymbol{\theta} - P_{\mathbf{K}}(\boldsymbol{\theta})\big) + E\big(P_{\mathbf{K}}(\boldsymbol{\theta}) - P_{\mathbf{K}}(\boldsymbol{\eta})\big) \geq E\big(P_{\mathbf{K}}(\boldsymbol{\theta}) - P_{\mathbf{K}}(\boldsymbol{\eta})\big)\ .
\end{aligned}$$

Thus, $D\psi_{\mathbf{K}}(\boldsymbol{\eta})[\boldsymbol{\theta} - \boldsymbol{\eta}] \leq \psi_{\mathbf{K}}(\boldsymbol{\theta}) - \psi_{\mathbf{K}}(\boldsymbol{\eta})$, i. e., $D\psi_{\mathbf{K}}$ is monotone and therefore $\psi_{\mathbf{K}}$ is convex. Finally, since $\mathbf{0} \in \mathbf{K}$ we have $\psi_{\mathbf{K}}(\boldsymbol{\theta}) = E(\boldsymbol{\theta}) - E\big(\boldsymbol{\theta} - P_{\mathbf{K}}(\boldsymbol{\theta})\big) \geq E(\boldsymbol{\theta}) - E(\boldsymbol{\theta} - \mathbf{0}) = 0$. □

The SQP method and linearized projections. Starting with $\boldsymbol{\sigma}^0 = \boldsymbol{\theta}$ and $\gamma^0 = 0$, the projection can be computed by the SQP method, i. e., in every iteration step we have to solve the corresponding KKT system

$$\begin{aligned}
\mathbf{0} = \boldsymbol{\sigma}^{k-1} - \boldsymbol{\theta} &+ \gamma^{k-1} \cdot \mathbb{C} : D\phi(\boldsymbol{\sigma}^{k-1}) \\
&+ \Delta\boldsymbol{\sigma}^k + \gamma^{k-1} \cdot \mathbb{C} : D^2\phi(\boldsymbol{\sigma}^{k-1}) : \Delta\boldsymbol{\sigma}^k + \Delta\gamma^k \cdot \mathbb{C} : D\phi(\boldsymbol{\sigma}^{k-1})\ , \\
\phi_k(\boldsymbol{\sigma}^k) \leq 0, &\quad \gamma^k \cdot \phi_k(\boldsymbol{\sigma}^k) = 0, \quad \gamma^k \geq 0\ ,
\end{aligned}$$

where $\phi_k(\boldsymbol{\sigma}) = \phi(\boldsymbol{\sigma}^{k-1}) + D\phi(\boldsymbol{\sigma}^{k-1}) : (\boldsymbol{\sigma} - \boldsymbol{\sigma}^{k-1})$ is the linearized flow rule. The new iterates are given by $\boldsymbol{\sigma}^k = \boldsymbol{\sigma}^{k-1} + \Delta\boldsymbol{\sigma}^k$ and $\gamma^k = \gamma^{k-1} + \Delta\gamma^k$.

The key observation for the construction of the new algorithm in Section 7.3 below is that the SQP step can be interpreted geometrically as the projection onto the half-space defined by the linearized flow rule

$$\mathbf{K}_k = \{\boldsymbol{\tau} \in \mathrm{Sym}(d) \colon \phi_k(\boldsymbol{\tau}) \leq 0\} \supset \mathbf{K}$$

with respect to a suitable adapted metric. Therefore, rearranging the first equation and defining $\mathbb{G}_k = \mathrm{id} + \gamma^{k-1} \cdot \mathbb{C} : D^2\phi(\boldsymbol{\sigma}^{k-1})$ gives

$$\mathbf{0} = \mathbb{G}_k : \boldsymbol{\sigma}^k - \boldsymbol{\theta} - \gamma^{k-1} \cdot \mathbb{C} : D^2\phi(\boldsymbol{\sigma}^{k-1}) : \boldsymbol{\sigma}^{k-1} + \gamma^k \cdot \mathbb{C} : D\phi(\boldsymbol{\sigma}^{k-1})\,.$$

Since ϕ is convex, $D^2\phi(\boldsymbol{\sigma}^{k-1})$ is positive semi-definite, and $\mathbb{G}_k$ can be inverted. Introducing $\mathbb{C}_k = \mathbb{G}_k^{-1} : \mathbb{C}$, $\boldsymbol{\theta}^k = \mathbb{G}_k^{-1} : \big(\boldsymbol{\theta} - \gamma^{k-1} \cdot \mathbb{C} : D^2\phi(\boldsymbol{\sigma}^{k-1}) : \boldsymbol{\sigma}^{k-1}\big)$ and using $D\phi_k(\boldsymbol{\sigma}^k) = D\phi(\boldsymbol{\sigma}^{k-1})$ rewrites the SQP step in the form

$$\mathbf{0} = \boldsymbol{\sigma}^k - \boldsymbol{\theta}^k + \gamma^k \cdot \mathbb{C}_k : D\phi_k(\boldsymbol{\sigma}^k) \ , \tag{6a}$$

$$\phi_k(\boldsymbol{\sigma}^k) \le 0, \quad \gamma^k \cdot \phi_k(\boldsymbol{\sigma}^k) = 0, \quad \gamma^k \ge 0 \ . \tag{6b}$$

Analogously to Lemma 1 we observe that $\boldsymbol{\sigma}^k = P_k(\boldsymbol{\theta}^k)$ where $P_k\colon \mathrm{Sym}(d) \longrightarrow \mathbf{K}_k$ is the orthogonal projection with respect to $e_k(\boldsymbol{\sigma}, \boldsymbol{\tau}) = \boldsymbol{\sigma} : \mathbb{C}_k^{-1} : \boldsymbol{\tau}$. Note that $\mathbb{C}_k$ is the algorithmic tangent modulus [**13**, Chap. 3.3.2 and Chap. 5.2.4].

Again, successively solving (6) for $k = 1, 2, 3, ...$ results in the SQP method for the evaluation of the projection, see Table 2.

PR0) Set $\boldsymbol{\sigma}^0 = \boldsymbol{\theta}$ and $\gamma^0 = 0$. Set $k = 1$.

PR1) Find $\boldsymbol{\sigma}^k$ and γ^k solving

$$\mathbf{0} = \boldsymbol{\sigma}^k - \boldsymbol{\theta}^k + \gamma^k \cdot \mathbb{C}_k : D\phi_k(\boldsymbol{\sigma}^k) \ ,$$
$$\phi_k(\boldsymbol{\sigma}^k) \le 0, \quad \gamma^k \cdot \phi_k(\boldsymbol{\sigma}^k) = 0, \quad \gamma^k \ge 0,$$

where $\phi_k(\boldsymbol{\sigma}) = \phi(\boldsymbol{\sigma}^{k-1}) + D\phi(\boldsymbol{\sigma}^{k-1}) : (\boldsymbol{\sigma} - \boldsymbol{\sigma}^{k-1})$,
$\mathbb{G}_k = \mathrm{id} + \gamma^{k-1} \cdot \mathbb{C} : D^2\phi(\boldsymbol{\sigma}^{k-1})$ and $\mathbb{C}_k = \mathbb{G}_k^{-1} : \mathbb{C}$, and
$\boldsymbol{\theta}^k = \mathbb{G}_k^{-1} : \big(\boldsymbol{\theta} - \gamma^{k-1} \cdot \mathbb{C} : D^2\phi(\boldsymbol{\sigma}^{k-1}) : \boldsymbol{\sigma}^{k-1}\big)$.

PR3) If $\boldsymbol{\sigma} - \boldsymbol{\theta} + \gamma \cdot \mathbb{C} : D\phi(\boldsymbol{\sigma})$ and $\max\{0, \phi(\boldsymbol{\sigma}^k)\}$ are small enough, stop.

PR4) Set $k := k + 1$ and go to PR1).

Table 2: SQP method for the approximation of the projection $\boldsymbol{\sigma} = P_{\mathbf{K}}(\boldsymbol{\theta})$ for a given trial stress $\boldsymbol{\theta} \in \mathrm{Sym}(d)$. In simple cases ($r = 1$ and von Mises flow rule) the algorithm stops after one iteration step.

Example: J2 plasticity. Let $r = 1$ and let $\phi(\boldsymbol{\sigma}) = |\,\mathrm{dev}(\boldsymbol{\sigma})| - K_0$ be the von Mises flow rule, where $\mathrm{dev}(\boldsymbol{\sigma}) = \boldsymbol{\sigma} - \frac{1}{3}\,\mathrm{trace}(\boldsymbol{\sigma})\mathbf{I}$. This gives

$$D\phi(\boldsymbol{\sigma}) = \frac{\mathrm{dev}(\boldsymbol{\sigma})}{|\,\mathrm{dev}(\boldsymbol{\sigma})|}\,, \qquad D^2\phi(\boldsymbol{\sigma}) : \boldsymbol{\eta} \ = \ \frac{\mathrm{dev}(\boldsymbol{\eta})}{|\,\mathrm{dev}(\boldsymbol{\sigma})|} - \frac{\mathrm{dev}(\boldsymbol{\sigma}) : \mathrm{dev}(\boldsymbol{\eta})}{|\,\mathrm{dev}(\boldsymbol{\sigma})|^2}\,\frac{\mathrm{dev}(\boldsymbol{\sigma})}{|\,\mathrm{dev}(\boldsymbol{\sigma})|}\,,$$

and $\mathbb{C} : D\phi(\boldsymbol{\sigma}) = 2\mu D\phi(\boldsymbol{\sigma})$, $\mathbb{C} : D^2\phi(\boldsymbol{\sigma}) = 2\mu D^2\phi(\boldsymbol{\sigma})$, $D^2\phi(\boldsymbol{\sigma}) : \boldsymbol{\sigma} = 0$. Moreover, direct computation yields

$$\Big(\mathrm{id} + 2\mu\gamma D^2\phi(\boldsymbol{\sigma})\Big)^{-1} \ = \ \mathrm{id} - \frac{2\mu\gamma|\,\mathrm{dev}(\boldsymbol{\sigma})|}{2\mu\gamma + |\,\mathrm{dev}(\boldsymbol{\sigma})|} D^2\phi(\boldsymbol{\sigma}) \ .$$

Thus, for given $\boldsymbol{\sigma}^{k-1}$ and γ^{k-1} we obtain

$$\boldsymbol{\theta}^k = \boldsymbol{\theta} - \frac{2\mu\gamma^{k-1}|\,\mathrm{dev}(\boldsymbol{\sigma}^{k-1})|}{2\mu\gamma^{k-1} + |\,\mathrm{dev}(\boldsymbol{\sigma}^{k-1})|} D^2\phi(\boldsymbol{\sigma}^{k-1}) : \boldsymbol{\theta}$$

and

$$P_k(\boldsymbol{\theta}^k) \ = \ \boldsymbol{\theta}^k - 2\mu\max\{0, \phi_k(\boldsymbol{\theta}^k)\}\frac{\mathrm{dev}(\boldsymbol{\theta}^k)}{|\,\mathrm{dev}(\boldsymbol{\theta}^k)|}\,, \qquad \gamma^k = \max\{0, \phi_k(\boldsymbol{\theta}^k)\} \ . \tag{7}$$

In this special example, the projection $P_{\mathbf{K}}$ is obtained in a single iteration step, i. e.,

$$P_{\mathbf{K}}(\boldsymbol{\theta}) \ = \ \boldsymbol{\theta} - 2\mu\max\{0, \phi(\boldsymbol{\theta})\}\frac{\mathrm{dev}(\boldsymbol{\theta})}{|\,\mathrm{dev}(\boldsymbol{\theta})|}\,, \qquad \gamma = \max\{0, \phi(\boldsymbol{\theta})\} \ , \tag{8}$$

see [**13**, Chap. 3.3.1].

4. The main principle in computational plasticity

Before we proceed with Prandtl-Reuss plasticity, we illustrate the standard approach in computational plasticity for the simple Hencky model of static infinitesimal plasticity. Therefore, let $\mathbf{V}$ be a finite element space of the displacements $\mathbf{u}$ (determining the linearized strains $\boldsymbol{\varepsilon}(\mathbf{u}) = \mathrm{sym}(D\mathbf{u}) \in \mathrm{Sym}(d)$), let $\boldsymbol{\Sigma}$ be the stress space and let $\boldsymbol{\Sigma}_{\mathbf{K}}$ be the convex set of stresses which are pointwise admissible in $\mathbf{K} \subset \mathrm{Sym}(d)$.

For a given load functional ℓ, the problem of static infinitesimal plasticity can be stated as follows: find a minimizer $\boldsymbol{\sigma} \in \boldsymbol{\Sigma}_{\mathbf{K}}$ of the dual energy

$$\mathcal{E}(\boldsymbol{\sigma}) = \int_\Omega E(\boldsymbol{\sigma})\, d\mathbf{x}$$

subject to the linear constraint

$$\int_\Omega \boldsymbol{\sigma} : \boldsymbol{\varepsilon}(\delta\mathbf{u})\, d\mathbf{x} = \ell(\delta\mathbf{u}), \qquad \delta\mathbf{u} \in \mathbf{V}\ .$$

The corresponding Lagrange functional is given by

$$\mathcal{L}(\boldsymbol{\sigma}, \mathbf{u}, \gamma) = \mathcal{E}(\boldsymbol{\sigma}) + \int_\Omega \gamma \cdot \phi(\boldsymbol{\sigma})\, d\mathbf{x} - \int_\Omega \boldsymbol{\sigma} : \boldsymbol{\varepsilon}(\mathbf{u})\, d\mathbf{x} + \ell(\mathbf{u})\ .$$

and every minimizer of the dual problem is characterized by the KKT-system

$$0 = \mathbb{C}^{-1} : \boldsymbol{\sigma} - \boldsymbol{\varepsilon}(\mathbf{u}) + \gamma \cdot D\phi(\boldsymbol{\sigma}), \tag{9a}$$

$$\phi(\boldsymbol{\sigma}) \le 0, \quad \gamma \cdot \phi(\boldsymbol{\sigma}) = 0, \quad \gamma \ge 0, \tag{9b}$$

$$0 = \int_\Omega \boldsymbol{\sigma} : \boldsymbol{\varepsilon}(\delta\mathbf{u})\, d\mathbf{x} - \ell(\delta\mathbf{u}), \qquad \delta\mathbf{u} \in \mathbf{V}(\mathbf{0})\ . \tag{9c}$$

Applying Lemma 1 to (9a) and (9b) gives $\boldsymbol{\sigma} = P_{\mathbf{K}}\big(\mathbb{C} : \boldsymbol{\varepsilon}(\mathbf{u})\big)$, and inserting into (9c) yields the nonlinear variational problem for the displacement $\mathbf{u} \in \mathbf{V}$

$$\int_\Omega P_{\mathbf{K}}\big(\mathbb{C} : \boldsymbol{\varepsilon}(\mathbf{u})\big) : \boldsymbol{\varepsilon}(\delta\mathbf{u})\, d\mathbf{x} = \ell(\delta\mathbf{u}), \qquad \delta\mathbf{u} \in \mathbf{V}\ .$$

This illustrates the main principle in nearly all methods in computational plasticity. We aim for developing a new class of solution methods with better mathematical properties.

5. Infinitesimal quasi-static perfect plasticity

We define the full equations of quasi-static plasticity, combining the global equilibrium equations in Ω, and the local pointwise equations for the stress-strain relation and the associated flow rule determined by the yield function ϕ.

Data. Let $\Omega \subset \mathbf{R}^d$ ($d = 2, 3$) be the reference configuration, and let $\Gamma_D \cup \Gamma_N = \partial\Omega$ be a decomposition of the boundary. We fix a time interval $[0, T]$.

The problem depends on the following data: a prescribed displacement vector

$$\mathbf{u}_D \colon \Gamma_D \times [0, T] \longrightarrow \mathbf{R}^d$$

for the essential boundary conditions on Γ_D and a load functional

$$\ell(t, \delta\mathbf{u}) = \int_\Omega \mathbf{b}(t) \cdot \delta\mathbf{u}\, d\mathbf{x} + \int_{\Gamma_N} \mathbf{t}_N(t) \cdot \delta\mathbf{u}\, d\mathbf{a}$$

depending on body force densities and traction force densities

$$\mathbf{b} \colon \Omega \times [0, T] \longrightarrow \mathbf{R}^d, \qquad \mathbf{t}_N \colon \Gamma_N \times [0, T] \longrightarrow \mathbf{R}^d\ .$$

The equations of infinitesimal plasticity. We want to determine displacements

$$\mathbf{u}\colon \overline{\Omega} \times [0,T] \longrightarrow \mathbf{R}^d \ ,$$

stresses

$$\boldsymbol{\sigma}\colon \Omega \times [0,T] \longrightarrow \mathrm{Sym}(d) \ ,$$

plastic strains

$$\boldsymbol{\varepsilon}_p\colon \Omega \times [0,T] \longrightarrow \mathrm{Sym}(d) \ ,$$

and a plastic multiplier

$$\lambda\colon \Omega \times [0,T] \longrightarrow \mathbf{R}^r$$

satisfying the essential boundary conditions

$$\mathbf{u}(\mathbf{x},t) = \mathbf{u}_D(\mathbf{x},t), \qquad (\mathbf{x},t) \in \Gamma_D \times [0,T] \ ,$$

the constitutive relation

$$\boldsymbol{\sigma}(\mathbf{x},t) = \mathbb{C} : \Big(\boldsymbol{\varepsilon}(\mathbf{u})(\mathbf{x},t) - \boldsymbol{\varepsilon}_p(\mathbf{x},t)\Big), \qquad (\mathbf{x},t) \in \Omega \times [0,T]$$

the equilibrium equations

$$\begin{aligned} -\operatorname{div}\boldsymbol{\sigma}(\mathbf{x},t) &= \mathbf{b}(\mathbf{x},t), \qquad (\mathbf{x},t) \in \Omega \times [0,T] \ , \\ \boldsymbol{\sigma}(\mathbf{x},t)\mathbf{n}(\mathbf{x}) &= \mathbf{t}_N(\mathbf{x},t), \qquad (\mathbf{x},t) \in \Gamma_N \times [0,T] \end{aligned}$$

(where $\mathbf{n}(\mathbf{x})$ denotes the outer unit normal vector on $\partial\Omega$), the flow rule

$$\frac{d}{dt}\boldsymbol{\varepsilon}_p(\mathbf{x},t) = \lambda(\mathbf{x},t) \cdot D\phi(\boldsymbol{\sigma}(\mathbf{x},t)) \ , \qquad (\mathbf{x},t) \in \Omega \times [0,T] \ , \tag{10}$$

and the complementary conditions (Karush-Kuhn-Tucker)

$$\lambda(\mathbf{x},t) \cdot \phi\big(\boldsymbol{\sigma}(\mathbf{x},t)\big) = 0, \ \ \lambda(\mathbf{x},t) \geq 0, \ \ \phi(\boldsymbol{\sigma}(\mathbf{x},t)) \leq 0, \quad (\mathbf{x},t) \in \Omega \times [0,T] \ . \tag{11}$$

6. Discrete infinitesimal plasticity

The discrete model is constructed in two steps. First, we introduce a spatial discretization based on finite elements for the displacements and Gauss point values for stresses and internal parameters. Then, the fully discrete model is obtained by a backward Euler method in time.

Discretization in space. Let $\mathbf{V} \subset C^{0,1}(\overline{\Omega}, \mathbf{R}^d)$ be a finite element space spanned by nodal basis functions. Let

$$\mathbf{V}(\mathbf{u}_D) = \{\mathbf{v} \in \mathbf{V}\colon \mathbf{v}(\mathbf{x}) = \mathbf{u}_D(\mathbf{x}) \text{ for } \mathbf{x} \in D\},$$

where $D \subset \Gamma_D$ is the set of all nodal points on Γ_D.

Let $\boldsymbol{\Xi} \subset \Omega$ be quadrature points and let $\omega_{\boldsymbol{\xi}}$ be corresponding quadrature weights such that

$$\int_\Omega \boldsymbol{\varepsilon}(\mathbf{v}) : \boldsymbol{\varepsilon}(\mathbf{w})\, d\mathbf{x} = \sum_{\boldsymbol{\xi}\in\boldsymbol{\Xi}} \omega_{\boldsymbol{\xi}}\, \boldsymbol{\varepsilon}(\mathbf{v})(\boldsymbol{\xi}) : \boldsymbol{\varepsilon}(\mathbf{w})(\boldsymbol{\xi})\,, \qquad \mathbf{v},\mathbf{w} \in \mathbf{V} \ .$$

We set $\boldsymbol{\Lambda} = \{\mu\colon \boldsymbol{\Xi} \longrightarrow \mathbf{R}^r\}$ and $\boldsymbol{\Sigma} = \{\boldsymbol{\tau}\colon \boldsymbol{\Xi} \longrightarrow \mathrm{Sym}(d)\}$. Let $\boldsymbol{\varepsilon}\colon \mathbf{V} \longrightarrow \boldsymbol{\Sigma}$ be given by $\boldsymbol{\varepsilon}(\mathbf{v})(\boldsymbol{\xi}) = \mathrm{sym}\,\big(D\mathbf{v}(\boldsymbol{\xi})\big)$. For given $\mathbf{u} \in \mathbf{V}$ this defines $\mathbb{C} : \boldsymbol{\varepsilon}(\mathbf{u}) \in \boldsymbol{\Sigma}$. In our notation, the integral is used also for the finite sums

$$\int_\Omega \boldsymbol{\sigma} : \boldsymbol{\varepsilon}\, d\mathbf{x} \ := \ \sum_{\boldsymbol{\xi}\in\boldsymbol{\Xi}} \omega_{\boldsymbol{\xi}}\, \boldsymbol{\sigma}(\boldsymbol{\xi}) : \boldsymbol{\varepsilon}(\boldsymbol{\xi}) \ .$$

The semi-discrete equations of infinitesimal plasticity. The semi-discrete problem which is discrete in space and continuous in time reads as follows: determine displacements

$$\mathbf{u}\colon [0,T] \longrightarrow \mathbf{V} \ ,$$

stresses

$$\boldsymbol{\sigma}\colon [0,T] \longrightarrow \boldsymbol{\Sigma} \ ,$$

plastic strains

$$\varepsilon_p\colon [0,T] \longrightarrow \boldsymbol{\Sigma} \ ,$$

and a plastic multiplier

$$\lambda\colon [0,T] \longrightarrow \boldsymbol{\Lambda}$$

satisfying the essential boundary conditions

$$\mathbf{u}(t) \in \mathbf{V}(\mathbf{u}_D(t)) \ , \qquad t \in [0,T] \ ,$$

the constitutive relation

$$\boldsymbol{\sigma}(\boldsymbol{\xi},t) = \mathbb{C} : \Big(\varepsilon(\mathbf{u})(\boldsymbol{\xi},t) - \varepsilon_p(\boldsymbol{\xi},t)\Big), \qquad (\boldsymbol{\xi},t) \in \boldsymbol{\Xi} \times [0,T]$$

(using $\boldsymbol{\sigma}(\boldsymbol{\xi},t) := \boldsymbol{\sigma}(t)(\boldsymbol{\xi})$ for $\boldsymbol{\sigma}(t) \in \boldsymbol{\Sigma}$), the equilibrium equation in weak form

$$\int_\Omega \boldsymbol{\sigma}(t) : \varepsilon(\delta\mathbf{u})\, d\mathbf{x} \quad = \quad \ell(t,\delta\mathbf{u}), \qquad t \in [0,T], \quad \delta\mathbf{u} \in \mathbf{V}(\mathbf{0}) \ ,$$

the flow rule

$$\frac{d}{dt}\varepsilon_p(\boldsymbol{\xi},t) = \lambda(\boldsymbol{\xi},t) \cdot D\phi(\boldsymbol{\sigma}(\boldsymbol{\xi},t)) \ , \qquad (\boldsymbol{\xi},t) \in \boldsymbol{\Xi} \times [0,T] \ ,$$

and the complementary conditions (Karush-Kuhn-Tucker)

$$\lambda(\boldsymbol{\xi},t) \cdot \phi\big(\boldsymbol{\sigma}(\boldsymbol{\xi},t)\big) = 0, \quad \lambda(\boldsymbol{\xi},t) \geq 0, \quad \phi(\boldsymbol{\sigma}(\boldsymbol{\xi},t)) \leq 0, \qquad (\boldsymbol{\xi},t) \in \Omega \times [0,T] \ .$$

Discretization in time. The model of incremental infinitesimal plasticity is obtained by a decomposition

$$0 = t_0 < t_1 < \cdots < t_N = T$$

of the time interval and the application of the backward Euler scheme: for $n = 1,2,3,...$ the next increment depends on the material history described by ε_p^{n-1} (starting with $\varepsilon_p^0 = \mathbf{0}$), the new load $\ell_n(\delta\mathbf{u}) = \ell(t_n,\delta\mathbf{u})$ and the new Dirichlet boundary values $\mathbf{u}_D^n = \mathbf{u}_D(t_n)$. We compute the displacement $\mathbf{u}^n \in \mathbf{V}(\mathbf{u}_D^n)$ satisfying the essential boundary conditions, the stress $\boldsymbol{\sigma}^n \in \boldsymbol{\Sigma}$, the plastic strain $\varepsilon_p^n \in \boldsymbol{\Sigma}$, and the plastic multiplier $\lambda^n \in \boldsymbol{\Lambda}$ satisfying the constitutive relation

$$\boldsymbol{\sigma}^n(\boldsymbol{\xi}) = \mathbb{C} : \Big(\varepsilon(\mathbf{u}^n)(\boldsymbol{\xi}) - \varepsilon_p^n(\boldsymbol{\xi})\Big), \qquad \boldsymbol{\xi} \in \boldsymbol{\Xi} \ , \tag{12}$$

the *equilibrium equation*

$$\int_\Omega \boldsymbol{\sigma}^n : \varepsilon(\delta\mathbf{u})\, d\mathbf{x} \quad = \quad \ell_n(\delta\mathbf{u}), \qquad \delta\mathbf{u} \in \mathbf{V}(\mathbf{0}) \ , \tag{13}$$

the discretized *flow rule*

$$\frac{1}{t_n - t_{n-1}} \Big(\varepsilon_p^n(\boldsymbol{\xi}) - \varepsilon_p^{n-1}(\boldsymbol{\xi})\Big) = \lambda^n(\boldsymbol{\xi}) \cdot D\phi(\boldsymbol{\sigma}^n(\boldsymbol{\xi})) \ , \qquad \boldsymbol{\xi} \in \boldsymbol{\Xi} \ ,$$

and the *complementary conditions*

$$\lambda^n(\boldsymbol{\xi}) \cdot \phi\big(\boldsymbol{\sigma}^n(\boldsymbol{\xi})\big) = 0, \quad \lambda^n(\boldsymbol{\xi}) \geq 0, \quad \phi(\boldsymbol{\sigma}^n(\boldsymbol{\xi})) \leq 0, \qquad \boldsymbol{\xi} \in \boldsymbol{\Xi} \ .$$

Since the problem is rate-independent, rescaling of the time parameter does not affect the model. Thus, we define $\gamma^n = (t_n - t_{n-1})\lambda^n \in \boldsymbol{\Lambda}$, i. e., the flow rule has the form

$$\varepsilon_p^n(\boldsymbol{\xi}) = \varepsilon_p^{n-1}(\boldsymbol{\xi}) + \gamma^n(\boldsymbol{\xi}) \cdot D\phi(\boldsymbol{\sigma}^n(\boldsymbol{\xi})) \ , \qquad \boldsymbol{\xi} \in \boldsymbol{\Xi} \ . \tag{14}$$

Together with (12) and (13), we can state the fully discrete problem in infinitesimal perfect plasticity: for given $\boldsymbol{\varepsilon}_p^{n-1} \in \boldsymbol{\Sigma}$ find $\boldsymbol{\sigma}^n \in \boldsymbol{\Sigma}$, $\mathbf{u}^n \in \mathbf{V}(\mathbf{u}_D^n)$ and $\gamma^n \in \boldsymbol{\Lambda}$ such that the equilibrium equation, the flow rule and the complementary conditions are satisfied

$$\text{(FR}_n) \qquad \boldsymbol{\sigma}^n(\boldsymbol{\xi}) = \mathbb{C} : \Big(\boldsymbol{\varepsilon}(\mathbf{u}^n)(\boldsymbol{\xi}) - \boldsymbol{\varepsilon}_p^{n-1}(\boldsymbol{\xi}) - \gamma^n(\boldsymbol{\xi}) \cdot D\phi(\boldsymbol{\sigma}^n(\boldsymbol{\xi}))\Big), \qquad \boldsymbol{\xi} \in \boldsymbol{\Xi}\,, \tag{15a}$$

$$\text{(CC}_n) \qquad \phi(\boldsymbol{\sigma}^n(\boldsymbol{\xi})) \le 0, \quad \gamma^n(\boldsymbol{\xi}) \cdot \phi\big(\boldsymbol{\sigma}^n(\boldsymbol{\xi})\big) = 0, \quad \gamma^n(\boldsymbol{\xi}) \ge 0, \qquad \boldsymbol{\xi} \in \boldsymbol{\Xi}\,, \tag{15b}$$

$$\text{(EE}_n) \qquad \int_\Omega \boldsymbol{\sigma}^n : \boldsymbol{\varepsilon}(\delta\mathbf{u})\, d\mathbf{x} = \ell_n(\delta\mathbf{u}), \qquad \delta\mathbf{u} \in \mathbf{V}(\mathbf{0})\,. \tag{15c}$$

For the next time step, $\boldsymbol{\varepsilon}_p^n$ is determined by the discretized flow rule (14).

The discrete dual problem in incremental plasticity. We study the dual minimization problem for a fixed time step from t_{n-1} to t_n and for given $\boldsymbol{\varepsilon}_p^{n-1} \in \boldsymbol{\Sigma}$. In order to incorporate the Dirichlet boundary conditions into the Lagrange parameter, we reformulate the equilibrium equation (15c) in the equivalent form

$$\int_\Omega \boldsymbol{\sigma}^n : \boldsymbol{\varepsilon}(\delta\mathbf{u})\, d\mathbf{x} - \int_{\Gamma_D} (\boldsymbol{\sigma}^n\mathbf{n}) \cdot \delta\mathbf{u}\, d\mathbf{a} = \ell_n(\delta\mathbf{u}), \qquad \delta\mathbf{u} \in \mathbf{V}(\mathbf{u}_D^n)\,. \tag{16}$$

The corresponding incremental dual energy is defined by

$$\mathcal{E}_n(\boldsymbol{\sigma}) = \int_\Omega E\big(\boldsymbol{\sigma} - \mathbb{C} : \boldsymbol{\varepsilon}_p^{n-1}\big)\, d\mathbf{x} - \int_{\Gamma_D} (\boldsymbol{\sigma}\mathbf{n}) \cdot \mathbf{u}_D^n\, d\mathbf{a}\,. \tag{17}$$

Then, the dual convex minimization problem reads as follows: find a minimizer $\boldsymbol{\sigma} \in \boldsymbol{\Sigma}$ of the dual energy $\mathcal{E}_n(\cdot)$ subject to the pointwise convex constraint $\boldsymbol{\sigma}(\boldsymbol{\xi}) \in \mathbf{K}$ for $\boldsymbol{\xi} \in \boldsymbol{\Xi}$ and the linear constraint (16).

THEOREM 3. *Assume that a strictly admissible stress state $\boldsymbol{\tau}^n \in \boldsymbol{\Sigma}$ exists, i. e.,*

$$\phi\big(\boldsymbol{\tau}^n(\boldsymbol{\xi})\big) < 0, \qquad \boldsymbol{\xi} \in \boldsymbol{\Xi}\,, \tag{18a}$$

$$\int_\Omega \boldsymbol{\tau}^n : \boldsymbol{\varepsilon}(\delta\mathbf{u})\, d\mathbf{x} = \ell_n(\delta\mathbf{u}), \qquad \delta\mathbf{u} \in \mathbf{V}(\mathbf{0})\,. \tag{18b}$$

Then, problem (15) *has a solution $(\boldsymbol{\sigma}^n, \mathbf{u}^n, \gamma^n) \in \boldsymbol{\Sigma} \times \mathbf{V}(\mathbf{u}_D^n) \times \boldsymbol{\Lambda}$. Moreover, $\boldsymbol{\sigma}^n$ is the unique minimizer of the dual convex minimization problem.*

PROOF. Since $\mathcal{E}^n(\cdot)$ is uniformly convex and since $\boldsymbol{\tau}^k$ is pointwise in $\mathbf{K}$ and satisfies (16), the admissible set is not empty and therefore a unique solution $\boldsymbol{\sigma}^n$ of the incremental dual problem exists. Moreover, since $\boldsymbol{\tau}^k$ is strictly admissible (i. e., the Slater condition is fulfilled), Lagrange multipliers $(\mathbf{u}^n, \gamma^n) \in \mathbf{V}(\mathbf{u}_D^n) \times \boldsymbol{\Lambda}$ with $\gamma^n \ge 0$ exist, such that $(\boldsymbol{\sigma}^n, \mathbf{u}^n, \gamma^n) \in \boldsymbol{\Sigma} \times \mathbf{V}(\mathbf{u}_D^n) \times \boldsymbol{\Lambda}$ is a saddle point of the Lagrange functional

$$\mathcal{L}^n(\boldsymbol{\sigma}, \mathbf{u}, \gamma) = \mathcal{E}^n(\boldsymbol{\sigma}) + \int_\Omega \gamma \cdot \phi(\boldsymbol{\sigma})\, d\mathbf{x} - \int_\Omega \boldsymbol{\sigma} : \boldsymbol{\varepsilon}(\mathbf{u})\, d\mathbf{x} + \int_{\Gamma_D} (\boldsymbol{\sigma}\mathbf{n}) \cdot \mathbf{u}\, d\mathbf{a} + \ell_n(\mathbf{u})\,.$$

Thus, $(\boldsymbol{\sigma}^n, \mathbf{u}^n, \gamma^n)$ is a critical point of the Lagrange functional: we have

$$\begin{aligned} D_{\boldsymbol{\sigma}}\mathcal{L}^n(\boldsymbol{\sigma}, \mathbf{u}, \gamma)[\delta\boldsymbol{\sigma}] &= \int_\Omega \boldsymbol{\sigma} : \mathbb{C}^{-1} : \delta\boldsymbol{\sigma}\, d\mathbf{x} - \int_\Omega \boldsymbol{\varepsilon}_p^{n-1} : \delta\boldsymbol{\sigma}\, d\mathbf{x} \\ &\quad + \int_\Omega \gamma \cdot D\phi(\boldsymbol{\sigma}) : \delta\boldsymbol{\sigma}\, d\mathbf{x} - \int_\Omega \delta\boldsymbol{\sigma} : \boldsymbol{\varepsilon}(\mathbf{u})\, d\mathbf{x}\,, \end{aligned}$$

and $D_{\boldsymbol{\sigma}}\mathcal{L}^n(\boldsymbol{\sigma}^n, \mathbf{u}^n, \gamma^n)[\delta\boldsymbol{\sigma}] = 0$ for all $\delta\boldsymbol{\sigma} \in \boldsymbol{\Sigma}$ is equivalent to

$$\mathbb{C}^{-1} : \boldsymbol{\sigma}^n(\boldsymbol{\xi}) - \boldsymbol{\varepsilon}_p^{n-1}(\boldsymbol{\xi}) + \gamma^n(\boldsymbol{\xi}) \cdot D\phi(\boldsymbol{\sigma}^n(\boldsymbol{\xi})) - \boldsymbol{\varepsilon}(\mathbf{u}^n)(\boldsymbol{\xi}) = \mathbf{0}, \qquad \boldsymbol{\xi} \in \boldsymbol{\Xi}\,.$$

Together with the admissibility in $\mathbf{K}$ and the equilibrium equation (16), this shows that (15) is equivalent to the KKT-system of the incremental dual minimization problem. □

7. Algorithms in computational plasticity

We discuss two classes of nonlinear solution methods for the discrete incremental problem (15):

a) The equations (FR_n) and (CC_n) describe the orthogonal projection of a suitably defined trial stress onto the admissible set of stresses. Inserting this projection into the equilibrium equation (EE_n) results in a nonlinear variational problem for the displacements which is solved by a generalized Newton method. Within every iteration step, the stress and the plastic parameter are defined by the local solution of (FR_n) and (CC_n) independently for each integration point.
This is the standard return algorithm in computational plasticity, often referred to as Radial Return or Closest Point Projection (see, e. g., [**13**]).
b) Linearizing the flow rule results in the KKT-system of a quadratic minimization problem. This defines the SQP method. The iterates solve the equilibrium equation together with linearizations ($\mathrm{FR}_{n,k}$) and ($\mathrm{CC}_{n,k}$) of flow the rule and the complementary condition. The iteration stops if (FR_n) and (CC_n) are satisfied up to sufficient accuracy.

REMARK 4. *In the special case of J2 plasticity with von Mises flow rule further variants are possible since the projection can be evaluated directly by* (8). *Eliminating* (15b) *in* (15) *yields*

$$(\mathrm{FR}'_n) \qquad \boldsymbol{\sigma}^n(\boldsymbol{\xi}) = \mathbb{C} : \Big(\boldsymbol{\varepsilon}(\mathbf{u}^n)(\boldsymbol{\xi}) - \boldsymbol{\varepsilon}_p^{n-1}(\boldsymbol{\xi}) - \max\{0, \phi(\boldsymbol{\sigma}^n)\} D\phi(\boldsymbol{\sigma}^n(\boldsymbol{\xi}))\Big), \ \boldsymbol{\xi} \in \Xi \ , \tag{19a}$$

$$(\mathrm{EE}'_n) \qquad \int_\Omega \boldsymbol{\sigma}^n : \boldsymbol{\varepsilon}(\delta\mathbf{u})\, d\mathbf{x} = \ell_n(\delta\mathbf{u}), \qquad \delta\mathbf{u} \in \mathbf{V}(\mathbf{0}) \ . \tag{19b}$$

The application of a generalized Newton method directly to the system (19) *is studied by Christensen* [**3**].

7.1. The projection method.

Defining the trial stress

$$\boldsymbol{\theta}_n(\mathbf{u}) = \mathbb{C} : \big(\boldsymbol{\varepsilon}(\mathbf{u}) - \boldsymbol{\varepsilon}_p^{n-1}\big) \tag{20}$$

rewrites (15a) and (15b) in the form

$$0 = \boldsymbol{\sigma}^n - \boldsymbol{\theta}_n(\mathbf{u}^n) - \gamma^n \cdot \mathbb{C} : D\phi(\boldsymbol{\sigma}^n), \tag{21a}$$

$$\phi(\boldsymbol{\sigma}^n) \le 0, \quad \gamma^n \cdot \phi\big(\boldsymbol{\sigma}^n\big) = 0, \quad \gamma^n \ge 0 \ . \tag{21b}$$

Lemma 1 ensures that equation (21) can be solved independently for every integration point $\boldsymbol{\xi} \in \Xi$ defining the projection

$$\boldsymbol{\sigma}^n = P_{\mathbf{K}}(\boldsymbol{\theta}_n(\mathbf{u}^n)) \ . \tag{22}$$

Inserting (20) and (22) into the equilibrium equation (15c) yields the nonlinear variational problem for the incremental problem in plasticity: for given $\boldsymbol{\varepsilon}_p^{n-1}$, find $\mathbf{u}^n \in \mathbf{V}(\mathbf{u}_D^n)$ such that

$$\int_\Omega P_{\mathbf{K}}\big(\mathbb{C} : (\boldsymbol{\varepsilon}(\mathbf{u}^n) - \boldsymbol{\varepsilon}_p^{n-1})\big) : \boldsymbol{\varepsilon}(\delta\mathbf{u})\, d\mathbf{x} = \ell_n[\delta\mathbf{u}], \qquad \delta\mathbf{u} \in \mathbf{V}(\mathbf{0}) \ . \tag{23}$$

LEMMA 5. *The incremental energy functional*

$$\mathcal{I}_n^{\mathrm{incr}}(\mathbf{u}) = \int_\Omega \psi_{\mathbf{K}}\big(\boldsymbol{\theta}_n(\mathbf{u})\big)\, d\mathbf{x} - \ell_n[\mathbf{u}], \qquad \mathbf{u} \in \mathbf{V}(\mathbf{u}_D^n) \tag{24}$$

is convex. Moreover, if a strictly admissible stress $\boldsymbol{\tau}^n \in \boldsymbol{\Sigma}$ satisfying (18) *exists, the functional* (24) *has a minimizer $\mathbf{u}^n \in \mathbf{V}(\mathbf{u}_D^n)$ which solves the variational equation* (23).

Note that in general the primal solution is not unique.

PROOF. The convexity of $\mathcal{I}_n^{\rm incr}(\cdot)$ follows from Lemma 2. Moreover, (4) gives

$$\begin{aligned} D\Big(\psi_{\mathbf{K}}\big(\boldsymbol{\theta}_n(\mathbf{u}^n)\big)\Big)[\delta\mathbf{u}] &= D\psi_{\mathbf{K}}\big(\boldsymbol{\theta}_n(\mathbf{u}^n)\big)\big[D\boldsymbol{\theta}_n(\mathbf{u}^n)[\delta\mathbf{u}]\big] \\ &= e\big(P_{\mathbf{K}}(\boldsymbol{\theta}_n(\mathbf{u}^n)), \mathbb{C}:\boldsymbol{\varepsilon}(\delta\mathbf{u})\big) = P_{\mathbf{K}}(\boldsymbol{\theta}_n(\mathbf{u}^n)):\boldsymbol{\varepsilon}(\delta\mathbf{u}) \end{aligned}$$

and therefore

$$D\mathcal{I}_n^{\rm incr}(\mathbf{u})[\delta\mathbf{u}] = \int_\Omega P_{\mathbf{K}}\big(\mathbb{C}:(\boldsymbol{\varepsilon}(\mathbf{u})-\boldsymbol{\varepsilon}_p^{n-1})\big):\boldsymbol{\varepsilon}(\delta\mathbf{u})\,d\mathbf{x} - \ell_n[\delta\mathbf{u}]\ .$$

If the assumptions of Theorem 3 are satisfied, a solution $(\boldsymbol{\sigma}^n,\gamma^n,\mathbf{u}^n)$ of (15) exists. Moreover, by (21) the primal solution $\mathbf{u}^n$ solves equation (23). Thus, $\mathbf{u}^n$ is a critical point of $\mathcal{I}_n^{\rm incr}(\cdot)$, and since $\mathcal{I}_n^{\rm incr}(\cdot)$ is convex, it is a minimizer. □

We apply a generalized Newton iteration to find a minimizer of $\mathcal{I}_n^{\rm incr}(\cdot)$ by computing a critical point of $F_n = D\mathcal{I}_n^{\rm incr}$ (i. e., by solving the equation $F_n(\mathbf{u}^n)=0$). For a given start iterate $\mathbf{u}^{n,0}\in\mathbf{V}(\mathbf{u}_D^n)$, find increments $\Delta\mathbf{u}^{n,k}\in\mathbf{V}(\mathbf{0})$ and damping parameters $s^{n,k}\in(0,1]$ with

$$0\in F_n(\mathbf{u}^{n,k-1}) + \partial F_n(\mathbf{u}^{n,k-1})\Delta\mathbf{u}^{n,k},\quad \mathbf{u}^{n,k}=\mathbf{u}^{n,k-1}+s^{n,k}\Delta\mathbf{u}^{n,k},\quad k=1,2,3,...$$

such that the sequence $\mathcal{I}_n^{\rm incr}(\mathbf{u}^{n,k})$ is decreasing.

Choosing the consistent tangent $\mathbb{C}^{n,k}\in\partial\big(P_{\mathbf{K}}(\boldsymbol{\theta}_n(\mathbf{u}^{n,k-1}))\big) = \partial P_{\mathbf{K}}\big(\boldsymbol{\theta}_n(\mathbf{u}^{n,k-1})\big):\mathbb{C}$ leads to a realization of the Newton step in the form

$$\int_\Omega \boldsymbol{\varepsilon}(\Delta\mathbf{u}^{n,k}):\mathbb{C}^{n,k}:\boldsymbol{\varepsilon}(\delta\mathbf{u})\,d\mathbf{x} = \ell_n[\delta\mathbf{u}] - \int_\Omega P_{\mathbf{K}}\big(\boldsymbol{\theta}_n(\mathbf{u}^{n,k-1})\big):\boldsymbol{\varepsilon}(\delta\mathbf{u})\,d\mathbf{x}\ . \tag{25}$$

Example: J2 plasticity. For $\phi(\boldsymbol{\sigma}) = |\operatorname{dev}(\boldsymbol{\sigma})| - K_0$ we obtain from (8)

$$\begin{aligned} \partial P_{\mathbf{K}}(\boldsymbol{\theta})[\boldsymbol{\tau}] &= \boldsymbol{\tau} - \partial\max\{0,\operatorname{dev}(\boldsymbol{\theta})| - K_0\}\frac{\operatorname{dev}(\boldsymbol{\theta}):\operatorname{dev}(\boldsymbol{\tau})}{|\operatorname{dev}(\boldsymbol{\theta})|}\frac{\operatorname{dev}(\boldsymbol{\theta})}{|\operatorname{dev}(\boldsymbol{\theta})|} \\ &\quad - \max\{0,|\operatorname{dev}(\boldsymbol{\theta})| - K_0\}\Big(\frac{\operatorname{dev}(\boldsymbol{\tau})}{|\operatorname{dev}(\boldsymbol{\theta})|} - \frac{\operatorname{dev}(\boldsymbol{\theta}):\operatorname{dev}(\boldsymbol{\tau})}{|\operatorname{dev}(\boldsymbol{\theta})|}\frac{\operatorname{dev}(\boldsymbol{\theta})}{|\operatorname{dev}(\boldsymbol{\theta})|^2}\Big)\ . \end{aligned}$$

7.2. The Lagrange-Newton method. Alternatively one can consider a nonlinear iteration for the full KKT-system (15), where the inequality $\phi(\boldsymbol{\sigma})\le 0$ is replaced by the non-smooth equality $\max\big\{0,\phi(\boldsymbol{\sigma})\big\}=0$: find $(\boldsymbol{\sigma}^n,\gamma^n,\mathbf{u}^n)\in\boldsymbol{\Sigma}\times\boldsymbol{\Lambda}\times\mathbf{V}(\mathbf{u}_D^n)$ with

$$\mathcal{F}^n\big(\boldsymbol{\sigma}^n,\gamma^n,\mathbf{u}^n\big) = 0\ ,$$

where

$$\mathcal{F}^n\big(\boldsymbol{\sigma},\gamma,\mathbf{u}\big) = \begin{pmatrix} \boldsymbol{\sigma} - \mathbb{C}:\big(\boldsymbol{\varepsilon}(\mathbf{u}) - \boldsymbol{\varepsilon}_p^{n-1} - \gamma\cdot D\phi(\boldsymbol{\sigma})\big) \\ \max\big\{0,\phi(\boldsymbol{\sigma})\big\} \\ \int_\Omega \boldsymbol{\sigma}:\boldsymbol{\varepsilon}[\cdot]\,d\mathbf{x} - \ell_n[\cdot] \end{pmatrix}\ .$$

A corresponding generalized Newton iteration

$$0\in\mathcal{F}^n\big(\boldsymbol{\sigma}^{n,k-1},\gamma^{n,k-1},\mathbf{u}^{n,k-1}\big) + \partial\mathcal{F}^n\big(\boldsymbol{\sigma}^{n,k-1},\gamma^{n,k-1},\mathbf{u}^{n,k-1}\big)\begin{pmatrix}\Delta\boldsymbol{\sigma}^{n,k}\\ \Delta\gamma^{n,k}\\ \Delta\mathbf{u}^{n,k}\end{pmatrix}$$

can be defined by a suitable active set strategy (using the techniques proposed in [**6**]), although in general $\partial\mathcal{F}^n\big(\boldsymbol{\sigma}^{n,k-1},\gamma^{n,k-1},\mathbf{u}^{n,k-1}\big)$ is not regular.

The algorithmic realization has the same structure as the projection method with the same formula for the consistent linearization and a modified right-hand side. Since this approach in general does not fulfill the complementary conditions (15b), we consider the corresponding SQP method.

7.3. The linearized projection method. The SQP method is obtained by inserting the linearized complementary conditions into the Lagrange-Newton iteration: for a given iterate $(\boldsymbol{\sigma}^{n-1}, \gamma^{n-1}, \mathbf{u}^{n-1}) \in \boldsymbol{\Sigma} \times \boldsymbol{\Lambda} \times \mathbf{V}(\mathbf{u}_D^n)$ define the linearized flow rule

$$\phi_{n,k}(\boldsymbol{\sigma}) = \phi(\boldsymbol{\sigma}^{n,k-1}) + D\phi(\boldsymbol{\sigma}^{n,k-1}) : (\boldsymbol{\sigma} - \boldsymbol{\sigma}^{n,k-1}) \tag{26}$$

and consider the following system: find $(\Delta\boldsymbol{\sigma}^n, \Delta\gamma^n, \Delta\mathbf{u}^n) \in \boldsymbol{\Sigma} \times \boldsymbol{\Lambda} \times \mathbf{V}(\mathbf{0})$ with

$$\begin{aligned}
0 &= \boldsymbol{\sigma}^{n,k-1} - \mathbb{C} : \Big(\boldsymbol{\varepsilon}(\mathbf{u}^{n,k-1}) - \boldsymbol{\varepsilon}_p^{n-1} - \gamma^{n,k-1} \cdot D\phi\big(\boldsymbol{\sigma}^{n,k-1}\big)\Big) \\
&\quad + \Delta\boldsymbol{\sigma}^{n,k} - \mathbb{C} : \Big(\boldsymbol{\varepsilon}(\Delta\mathbf{u}^{n,k}) - \Delta\gamma^{n,k} \cdot D\phi\big(\boldsymbol{\sigma}^{n,k-1}\big) - \gamma^{n,k-1} \cdot D^2\phi\big(\boldsymbol{\sigma}^{n,k-1}\big) : \Delta\boldsymbol{\sigma}^{n,k}\Big)\,, \\
&\phi_{n,k}\big(\boldsymbol{\sigma}^{n,k}\big) \le 0, \quad \gamma^{n,k} \cdot \phi_{n,k}\big(\boldsymbol{\sigma}^{n,k}\big) = 0, \quad \gamma^{n,k} \ge 0\,, \\
0 &= \int_\Omega \boldsymbol{\sigma}^{n,k-1} : \boldsymbol{\varepsilon}(\delta\mathbf{u})\,d\mathbf{x} - \ell_n(\delta\mathbf{u}) + \int_\Omega \Delta\boldsymbol{\sigma}^n : \boldsymbol{\varepsilon}(\delta\mathbf{u})\,d\mathbf{x}, \qquad \delta\mathbf{u} \in \mathbf{V}(\mathbf{0})
\end{aligned}$$

with $(\boldsymbol{\sigma}^n, \gamma^n, \mathbf{u}^n) = (\boldsymbol{\sigma}^{n-1}, \gamma^{n-1}, \mathbf{u}^{n-1}) + (\Delta\boldsymbol{\sigma}^n, \Delta\gamma^n, \Delta\mathbf{u}^n)$. This can be rewritten as

$$(\mathrm{FR}_{n,k}) \qquad 0 = \boldsymbol{\sigma}^{n,k} - \mathbb{C} : \Big(\boldsymbol{\varepsilon}(\mathbf{u}^{n,k}) - \boldsymbol{\varepsilon}_p^{n-1} - \gamma^{n,k} \cdot D\phi\big(\boldsymbol{\sigma}^{n,k-1}\big) - \gamma^{n,k-1} \cdot D^2\phi\big(\boldsymbol{\sigma}^{n,k-1}\big) : (\boldsymbol{\sigma}^{n,k} - \boldsymbol{\sigma}^{n,k-1})\Big)\,, \tag{28a}$$

$$(\mathrm{CC}_{n,k}) \qquad \phi_{n,k}\big(\boldsymbol{\sigma}^{n,k}\big) \le 0, \quad \gamma^{n,k} \cdot \phi_{n,k}\big(\boldsymbol{\sigma}^{n,k}\big) = 0, \quad \gamma^{n,k} \ge 0\,, \tag{28b}$$

$$(\mathrm{EE}_{n,k}) \qquad \int_\Omega \boldsymbol{\sigma}^{n,k} : \boldsymbol{\varepsilon}(\delta\mathbf{u})\,d\mathbf{x} = \ell_n(\delta\mathbf{u}), \qquad \delta\mathbf{u} \in \mathbf{V}(\mathbf{0})\ . \tag{28c}$$

The standard return algorithm can be adapted to this system as follows. Since ϕ is convex, $D^2\phi$ is positive semi-definite and therefore $\mathbb{C}_{n,k} = \big(\,\mathrm{id} + \gamma^{n,k-1} \cdot \mathbb{C} : D^2\phi(\boldsymbol{\sigma}^{n,k-1})\big)^{-1} : \mathbb{C}$ is well-defined. Introducing the modified trial stress

$$\boldsymbol{\theta}_{n,k}(\mathbf{u}) = \mathbb{C}_{n,k} : \Big(\boldsymbol{\varepsilon}(\mathbf{u}) - \boldsymbol{\varepsilon}_p^{n-1} + \gamma^{n,k-1} \cdot D^2\phi\big(\boldsymbol{\sigma}^{n,k-1}\big) : \boldsymbol{\sigma}^{n,k-1}\Big)$$

and using $D\phi(\boldsymbol{\sigma}^{n,k-1}) = D\phi_{n,k}(\boldsymbol{\sigma}^{n,k})$ rewrites (28a) and (28b) in the form

$$0 = \boldsymbol{\sigma}^{n,k} - \boldsymbol{\theta}_{n,k}(\mathbf{u}^{n,k}) - \gamma^{n,k} \cdot \mathbb{C}_{n,k} : D\phi_{n,k}(\boldsymbol{\sigma}^{n,k}), \tag{29a}$$

$$\phi_{n,k}\big(\boldsymbol{\sigma}^{n,k}\big) \le 0, \quad \gamma^{n,k} \cdot \phi_{n,k}\big(\boldsymbol{\sigma}^{n,k}\big) = 0, \quad \gamma^{n,k} \ge 0\ . \tag{29b}$$

Again, Lemma 1 guarantees that equation (29) can be solved independently for every integration point $\boldsymbol{\xi} \in \boldsymbol{\Xi}$. We have

$$\boldsymbol{\sigma}^{n,k} = P_{n,k}\big(\boldsymbol{\theta}_{n,k}(\mathbf{u}^{n,k})\big)\,, \tag{30}$$

where $P_{n,k}\colon \mathrm{Sym}(d) \longrightarrow \mathbf{K}_{n,k}$ is the orthogonal projection onto the half-space

$$\mathbf{K}_{n,k} = \{\boldsymbol{\tau} \in \mathrm{Sym}(d)\colon \phi_{n,k}(\boldsymbol{\tau}) \le 0\} \supset \mathbf{K}$$

with respect to the inner product $e_{n,k}(\boldsymbol{\sigma}, \boldsymbol{\tau}) = \boldsymbol{\sigma} : (\mathbb{C}_{n,k})^{-1} : \boldsymbol{\tau}$. The associated energy is denoted by $E_{n,k}(\boldsymbol{\sigma}) = \frac{1}{2} e_{n,k}(\boldsymbol{\sigma}, \boldsymbol{\sigma})$, and the corresponding convex potential is given by $\psi_{n,k}(\boldsymbol{\sigma}) = E_{n,k}(\boldsymbol{\sigma}) - E_{n,k}(\boldsymbol{\sigma} - P_{n,k}(\boldsymbol{\sigma}))$.

Now inserting (30) into the equilibrium equation (28c) yields a nonlinear variational problem for the SQP step: for given iterates $(\boldsymbol{\sigma}^{n,k-1}, \gamma^{n,k-1})$ find $\mathbf{u}^{n,k} \in \mathbf{V}(\mathbf{u}_D^n)$ such that

$$\int_\Omega P_{n,k}\big(\boldsymbol{\theta}_{n,k}(\mathbf{u}^{n,k})\big) : \boldsymbol{\varepsilon}(\delta\mathbf{u})\,d\mathbf{x} = \ell_n[\delta\mathbf{u}], \qquad \delta\mathbf{u} \in \mathbf{V}(\mathbf{0})\ . \tag{31}$$

LEMMA 6. *The primal energy functional for the linearized projection step*

$$\mathcal{I}_{n,k}^{\mathrm{incr}}(\mathbf{u}) = \int_\Omega \psi_{n,k}\big(\boldsymbol{\theta}_{n,k}(\mathbf{u})\big)\,d\mathbf{x} - \ell_n[\mathbf{u}], \qquad \mathbf{u} \in \mathbf{V}(\mathbf{u}_D^n) \tag{32}$$

is convex. Moreover, if a strictly admissible stress satisfying (18) *exists, the functional* (32) *has a minimizer* $\mathbf{u}^{n,k} \in \mathbf{V}(\mathbf{u}_D^n)$ *which solves the variational equation* (31).

PROOF. The quadratic dual energy functional for the linearized projection step is given by

$$\mathcal{E}_{n,k}(\boldsymbol{\sigma}) = \int_\Omega E_{n,k}\Big(\boldsymbol{\sigma} - \mathbb{C}_{n,k} : \big(\boldsymbol{\varepsilon}_p^{n-1} - \gamma^{n,k-1} \cdot D^2\phi(\boldsymbol{\sigma}^{n,k-1}) : \boldsymbol{\sigma}^{n,k-1}\big)\Big)\, d\mathbf{x} - \int_{\Gamma_D} (\boldsymbol{\sigma}\mathbf{n}) \cdot \mathbf{u}_D^n \, d\mathbf{a} ,$$

and the SQP step can be formulated as follows: find a minimizer $\boldsymbol{\sigma}^{n,k}$ of $\mathcal{E}_{n,k}(\cdot)$ subject to the constraints $\boldsymbol{\sigma}(\boldsymbol{\xi}) \in \mathbf{K}_{n,k}$ for $\boldsymbol{\xi} \in \boldsymbol{\Xi}$ and the equilibrium equation (16). Since $\mathbf{K} \subset \mathbf{K}_{n,k}$, this minimization problem is also strictly admissible. Therefore, there exists a minimizer $\boldsymbol{\sigma}^{n,k}$ of $\mathcal{E}_{n,k}(\cdot)$ and Lagrange parameters $(\gamma^{n,k}, \mathbf{u}^{n,k})$ such that $(\boldsymbol{\sigma}^{n,k}, \gamma^{n,k}, \mathbf{u}^{n,k})$ is a solution of the corresponding KKT-system (28). Thus, $\mathbf{u}^{n,k}$ solves (31), and analogously to Lemma 5 we can show that $\mathbf{u}^{n,k}$ is a critical point and therefore a minimizer of $\mathcal{I}_{n,k}^{\text{incr}}(\cdot)$.
Moreover, since $\mathcal{E}_{n,k}(\cdot)$ is uniformly convex, the minimizer $\boldsymbol{\sigma}^{n,k}$ is unique. □

The SQP method is now realized by the linearized projection algorithm: for suitable starting iterates $(\boldsymbol{\sigma}^{n,0}, \gamma^{n,0})$, compute for $k = 1, 2, 3, ...$ a minimizer $\mathbf{u}^{n,k}$ of $I_{n,k}^{\text{incr}}(\cdot)$. Then, set

$$\boldsymbol{\sigma}^{n,k} = P_{n,k}(\boldsymbol{\theta}(\mathbf{u}^{n,k})), \qquad \gamma^{n,k} = \frac{\max\big\{0, \phi_{n,k}(\boldsymbol{\theta}_{n,k}(\mathbf{u}^{n,k}))\big\}}{D\phi(\boldsymbol{\sigma}^{n,k-1}) : \mathbb{C}_{n,k} : D\phi(\boldsymbol{\sigma}^{n,k-1})} ; \tag{33}$$

together $(\boldsymbol{\sigma}^{n,k}, \mathbf{u}^{n,k}, \gamma^{n,k})$ solve (28).

Since $\mathbf{u}^{n,k}$ is a critical point of $F_{n,k} = D\mathcal{I}_{n,k}^{\text{incr}}$, we use a generalized Newton method to solve the nonlinear variational problem (31): for a given start iterate $\mathbf{u}^{n,k,0} \in \mathbf{V}(\mathbf{u}_D^n)$ find increments $\Delta\mathbf{u}^{n,k,m} \in \mathbf{V}(\mathbf{0})$ and damping parameters $s^{n,k,m} \in (0,1]$ with

$$0 \in F_{n,k}(\mathbf{u}^{n,k,m-1}) + \partial F_{n,k}(\mathbf{u}^{n,k,m-1})\Delta\mathbf{u}_{n,k,m} ,$$

and $\mathbf{u}^{n,k,m} = \mathbf{u}^{n,k,m-1} + s_{n,k,m}\Delta\mathbf{u}^{n,k,m}$ for $m = 1, 2, 3, ...$ such that the sequence $\mathcal{I}_{n,k}^{\text{incr}}(\mathbf{u}^{n,k,m})$ is decreasing.

The realization of the Newton step requires the choice of a consistent tangent $\mathbb{C}^{n,k,m} \in \partial\big(P_{\mathbf{K}}(\boldsymbol{\theta}(\mathbf{u}^{n,k,m-1}))\big) = \partial P_{\mathbf{K}}\big(\boldsymbol{\theta}(\mathbf{u}^{n,k,m-1})\big) : \mathbb{C}_{n,k}$ and results in a linear problem of the form

$$\int_\Omega \boldsymbol{\varepsilon}(\Delta\mathbf{u}^{n,k,m}) : \mathbb{C}^{n,k,m} : \boldsymbol{\varepsilon}(\delta\mathbf{u})\, d\mathbf{x} = \ell_n[\delta\mathbf{u}] - \int_\Omega P_{n,k}\big(\boldsymbol{\theta}_{n,k}(\mathbf{u}^{n,k,m-1})\big) : \boldsymbol{\varepsilon}(\delta\mathbf{u})\, d\mathbf{x} . \tag{34}$$

Example: J2 plasticity. For $\phi(\boldsymbol{\sigma}) = |\operatorname{dev}(\boldsymbol{\sigma})| - K_0$ we obtain from (7)

$$\partial P_{n,k}(\boldsymbol{\theta})[\boldsymbol{\tau}] \quad = \quad \boldsymbol{\tau} - \partial \max\{0, \operatorname{dev}(\boldsymbol{\theta})| - K_0\} \frac{\operatorname{dev}(\boldsymbol{\theta}) : \operatorname{dev}(\boldsymbol{\tau})}{|\operatorname{dev}(\boldsymbol{\theta})|} \frac{\operatorname{dev}(\boldsymbol{\theta})}{|\operatorname{dev}(\boldsymbol{\theta})|} .$$

A short comparison. Algorithmically, the realization of the projection method (25) and the realization of the SQP method via linearized projections (34) have the same structure using different projections, trial stresses and consistent tangents, cf. Table 3.

Conceptually, both algorithms follow a different strategy. The projection method iterates along admissible $\boldsymbol{\sigma}^{n,k} = P_{\mathbf{K}}\big(\boldsymbol{\theta}_n(\mathbf{u}^{n,k-1})\big) \in \mathbf{K}$ until the equilibrium is reached (cf. Figure 1), whereas the SQP method iterates along $\boldsymbol{\sigma}^{n,k,m} = P_{n,k}\big(\boldsymbol{\theta}_{n,k}(\mathbf{u}^{n,k,m-1})\big) \in \mathbf{K}_{n,k}$ satisfying the equilibrium equation until the admissible set is reached (cf. Figure 2).

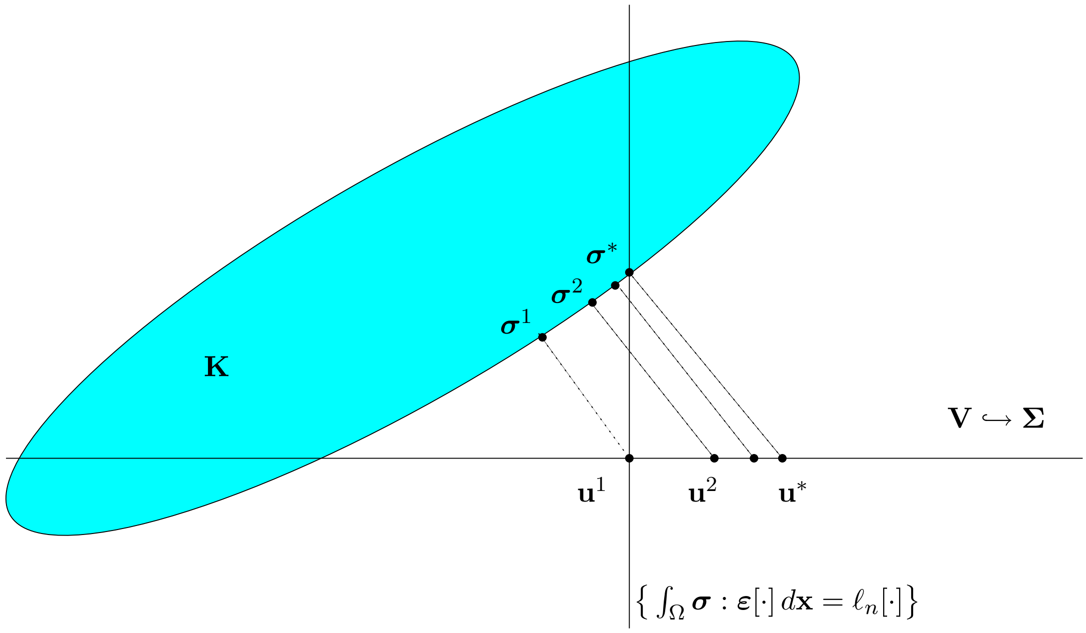

Figure 1: Illustration of the projection method for $\boldsymbol{\varepsilon}_p = \mathbf{0}$: find a displacement vector $\mathbf{u} \in \mathbf{V}$ such that the orthogonal projection onto $\mathbf{K}$ of the trial stress $\boldsymbol{\theta}$ yields the admissible stress $\boldsymbol{\sigma}$ in the intersection of the convex set $\mathbf{K}$ and the affine space of stress states satisfying the equilibrium condition (for this illustration we identify the displacements $\mathbf{u}$ with their associated trial stress $\boldsymbol{\theta}(\mathbf{u})$).

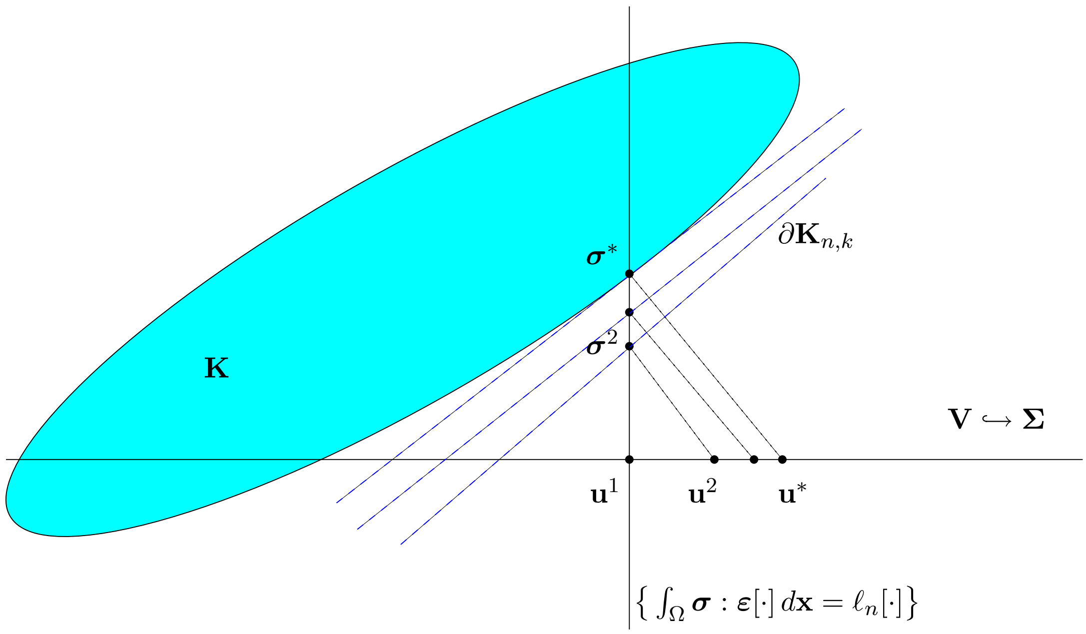

Figure 2: Illustration of the SQP method for $\boldsymbol{\varepsilon}_p = \mathbf{0}$: in every SQP step, find a displacement $\mathbf{u}^{n,k}$ such that the orthogonal projection onto the half-space $\mathbf{K}_{n,k}$ defined by the linearized linearized flow rule $\phi_{n,k}$ satisfies the equilibrium equation.

Projection method	**Linearized projection method (SQP)**
P0) Set $\boldsymbol{\varepsilon}_p^0 = \mathbf{0}$, $n = 1$.	S0) Set $\boldsymbol{\varepsilon}_p^0 = \boldsymbol{\sigma}^0 = \mathbf{0}$, $\gamma^0 = 0$, $n = 1$.
P1) Set $\mathbf{u}^{n,0} = \mathbf{u}^{n-1}$. Then, set the Dirichlet boundary values $\mathbf{u}^{n,0}(\mathbf{x}) = \mathbf{u}_D^n(\mathbf{x}), \quad \mathbf{x} \in D.$ Set $k = 1$.	S1) Set $\mathbf{u}^{n,0} = \mathbf{u}^{n-1}$, $\boldsymbol{\sigma}^{n,0} = \boldsymbol{\sigma}^{n-1}$, and $\gamma^{n,0} = \gamma^{n-1}$ Then, set the Dirichlet boundary values $\mathbf{u}^{n,0}(\mathbf{x}) = \mathbf{u}_D^n(\mathbf{x}), \quad \mathbf{x} \in D.$ Set $k = 1$.
	S2) Set $\mathbf{u}^{n,k,0} = \mathbf{u}^{n,k-1}$ and set $m = 1$.
P2) Compute the trial stress, the orthogonal projection $\boldsymbol{\sigma}^{n,k} = P_{\mathbf{K}}(\boldsymbol{\theta}_n(\mathbf{u}^{n,k-1}))$ and $\gamma^{k,n}$, evaluate the residual $R_{n,k}[\delta\mathbf{u}] = \ell^n(\delta\mathbf{u}) - \int_\Omega \boldsymbol{\sigma}^{n,k} : \boldsymbol{\varepsilon}(\delta\mathbf{u})\,d\mathbf{x}$.	S3) Compute the trial stress, the linearized projection $\boldsymbol{\sigma}^{n,k,m} = P_{n,k}(\boldsymbol{\theta}_{n,k}(\mathbf{u}^{n,k,m-1}))$ and $\gamma^{k,n,m}$, evaluate the residual $R_{n,k,m}[\delta\mathbf{u}] = \ell^n(\delta\mathbf{u}) - \int_\Omega \boldsymbol{\sigma}^{n,k,m} : \boldsymbol{\varepsilon}(\delta\mathbf{u})\,d\mathbf{x}$.
P3) If $\|R_{n,k}\|$ is not small enough, go to P5).	S4) If $\|R_{n,k,m}\|$ is not small enough, go to S8).
	S5) Set $\mathbf{u}^{n,k} = \mathbf{u}^{n,k,m}$, $\boldsymbol{\sigma}^{n,k} = \boldsymbol{\sigma}^{n,k,m}$, and $\gamma^{n,k} = \gamma^{n,k,m}$.
	S6) If the norm of $\boldsymbol{\sigma}^{n,k} - \mathbb{C} : (\boldsymbol{\varepsilon}(\mathbf{u}^{n,k}) - \boldsymbol{\varepsilon}_p^{n-1} - \gamma^{n,k} \cdot D\phi(\boldsymbol{\sigma}^{n,k}))$ is not small enough, set $k := k + 1$, and go to S2).
P4) Set $\mathbf{u}^n = \mathbf{u}^{n,k}$, $\boldsymbol{\sigma}^n = \boldsymbol{\sigma}^{n,k}$, $\gamma^n = \gamma^{n,k}$, $\boldsymbol{\varepsilon}_p^n = \boldsymbol{\varepsilon}_p^{n-1} + \gamma^n \cdot D\phi(\boldsymbol{\sigma}^n)$. Set $n := n + 1$ and go to P1).	S7) Set $\mathbf{u}^n = \mathbf{u}^{n,k}$, $\boldsymbol{\sigma}^n = \boldsymbol{\sigma}^{n,k}$, $\gamma^n = \gamma^{n,k}$, $\boldsymbol{\varepsilon}_p^n = \boldsymbol{\varepsilon}_p^{n-1} + \gamma^n \cdot D\phi(\boldsymbol{\sigma}^n)$. Set $n := n + 1$ and go to S1).
P5) Compute $\mathbb{C}^{n,k} \in \partial P_{\mathbf{K}}(\boldsymbol{\theta}_n(\mathbf{u}^{n,k-1})) : \mathbb{C}$ and compute $\Delta\mathbf{u}^{n,k}$ such that $\int_\Omega \boldsymbol{\varepsilon}(\Delta\mathbf{u}^{n,k}) : \mathbb{C}^{n,k} : \boldsymbol{\varepsilon}(\delta\mathbf{u})\,d\mathbf{x} = R_{n,k}[\delta\mathbf{u}]$. Determine a suitable damping factor $s^{n,k} \in (0, 1]$, set $\mathbf{u}^{n,k} = \mathbf{u}^{n,k-1} + s^{n,k}\Delta\mathbf{u}^{n,k}$. Set $k := k + 1$ and go to P2).	S8) Compute $\mathbb{C}^{n,k,m} \in \partial P_{n,k}(\boldsymbol{\theta}_{n,k}(\mathbf{u}^{n,k,m-1})) : \mathbb{C}_{n,k}$ and compute $\Delta\mathbf{u}^{n,k,m}$ such that $\int_\Omega \boldsymbol{\varepsilon}(\Delta\mathbf{u}^{n,k,m}) : \mathbb{C}^{n,k,m} : \boldsymbol{\varepsilon}(\delta\mathbf{u})\,d\mathbf{x} = R_{n,k,m}[\delta\mathbf{u}]$. Determine a suitable damping factor $s^{n,k,m} \in (0, 1]$, set $\mathbf{u}^{n,k,m} = \mathbf{u}^{n,k,m-1} + s^{n,k,m}\Delta\mathbf{u}^{n,k,m}$. Set $m := m + 1$ and go to S3).

Table 3: Comparison of the algorithmic steps for the projection method and the SQP method using linearized projections. For the SQP method, the additional step S6) is required to control the convergence of the flow rule. On the other hand, the nonlinear quadratic minimization problems of the SQP steps are simpler than the fully nonlinear problem in incremental plasticity. The realization of a specific model requires only formulae for the (linearized) trial stress, projection and consistent tangent (see Table 4 for J2 plasticity).

Projection method: compute $\boldsymbol{\theta}^{n,k}, \boldsymbol{\eta}^{n,k}, \gamma^{n,k}, \boldsymbol{\sigma}^{n,k}, \mathbb{C}^{n,k}$ with fixed $\mathbb{C}, P_{\mathbf{K}}$

$$\begin{aligned}
\boldsymbol{\theta}^{n,k} &= \boldsymbol{\theta}_n(\mathbf{u}^{n,k-1}) = \mathbb{C} : \big(\boldsymbol{\varepsilon}(\mathbf{u}^{n,k-1}) - \boldsymbol{\varepsilon}_p^{n-1}\big) \\
\boldsymbol{\eta}^{n,k} &= \frac{\mathrm{dev}(\boldsymbol{\theta}^{n,k})}{|\,\mathrm{dev}(\boldsymbol{\theta}^{n,k})|} \\
\gamma^{n,k} &= \max\{0, |\,\mathrm{dev}(\boldsymbol{\theta}^{n,k})| - K_0\} \\
\boldsymbol{\sigma}^{n,k} &= P_{\mathbf{K}}(\boldsymbol{\theta}^{n,k}) = \boldsymbol{\theta}^{n,k} - 2\mu\gamma^{n,k}\boldsymbol{\eta}^{n,k} \\
\mathbb{C}^{n,k} &= \mathbb{C} - 2\mu\,\mathrm{sgn}(\gamma^{n,k})\,\boldsymbol{\eta}^{n,k}\otimes\boldsymbol{\eta}^{n,k} - \frac{2\mu\gamma^{n,k}}{|\,\mathrm{dev}(\boldsymbol{\theta}^{n,k})|}\Big(\mathrm{dev} - \boldsymbol{\eta}^{n,k}\otimes\boldsymbol{\eta}^{n,k}\Big)
\end{aligned}$$

SQP method: compute $\boldsymbol{\theta}^{n,k,m}, \gamma^{n,k,m}, \boldsymbol{\sigma}^{n,k,m}, \mathbb{C}^{n,k,m}$ with modified $\boldsymbol{\eta}_{n,k}, \mathbb{C}_{n,k}, P_{n,k}$

$$\begin{aligned}
\boldsymbol{\eta}_{n,k} &= \frac{\mathrm{dev}(\boldsymbol{\sigma}^{n,k-1})}{|\,\mathrm{dev}(\boldsymbol{\sigma}^{n,k-1})|} \\
\mathbb{C}_{n,k} &= \mathbb{C} - 2\mu\frac{2\mu\gamma^{n,k-1}}{2\mu\gamma^{n,k-1} + |\,\mathrm{dev}(\boldsymbol{\sigma}^{n,k-1})|}\Big(\mathrm{dev} - \boldsymbol{\eta}_{n,k}\otimes\boldsymbol{\eta}_{n,k}\Big) \\
\boldsymbol{\theta}^{n,k,m} &= \boldsymbol{\theta}_{n,k}(\mathbf{u}^{n,k,m-1}) = \mathbb{C}_{n,k} : \big(\boldsymbol{\varepsilon}(\mathbf{u}^{n,k,m-1}) - \boldsymbol{\varepsilon}_p^{n-1}\big) \\
\gamma^{n,k,m} &= \max\{0, \phi(\boldsymbol{\theta}^{n,k,m}) + \boldsymbol{\eta}_{n,k} : \boldsymbol{\theta}^{n,k,m}\} \\
\boldsymbol{\sigma}^{n,k,m} &= P_{n,k}(\boldsymbol{\theta}^{n,k,m}) = \boldsymbol{\theta}^{n,k,m} - 2\mu\gamma^{n,k,m}\boldsymbol{\eta}_{n,k} \\
\mathbb{C}^{n,k,m} &= \mathbb{C}_{n,k} - 2\mu\,\mathrm{sgn}(\gamma^{n,k,m})\,\boldsymbol{\eta}_{n,k}\otimes\boldsymbol{\eta}_{n,k}
\end{aligned}$$

Table 4: Collection of the formulae for the evaluation of (linearized) trial stress, projection and consistent tangent for J2 plasticity. Here we use the signum function defined by $\mathrm{sgn}(\gamma) = 0$ for $\gamma = 0$ and $\mathrm{sgn}(\gamma) = 1$ for $\gamma > 0$.

8. Numerical experiment

We study the performance of the two algorithms for a benchmark problem in infinitesimal perfect plasticity (see **[9]**). The computations are realized in the finite element code M++ **[16]** supporting parallel multigrid methods.

For the benchmark problem we use the following material parameters: the elastic properties are determined by the Poisson ratio $\nu = 0.29$ and Young modulus $E = 206900.00[\mathrm{N/mm}^2]$ defining the Lamé parameters $\mu = E/(2(1+\nu))$ and $\lambda = E\nu/((1+\nu)(1-2\nu))$. Plasticity is determined by the yield stress $K_0 = 450.00[\mathrm{N/mm}^2]$. Geometry and boundary conditions are illustrated in Figure 3: the reference domain $\Omega = (0,10)\times(0,10)\setminus B_1(10,0)$ describes a quarter of a rectangle with a circular hole. The Dirichlet data arising by symmetry are given by

$$u_1(10, x_2) = 0, \quad x_2 \in (1,10), \qquad\qquad u_2(x_1, 0) = 0, \quad x_1 \in (0,9)\,,$$

and a load functional depending linearly on $t \geq 0$ is given by $\ell(t,\mathbf{v}) = 100\,t\int_0^{10}\mathbf{v}(x_1,10)\,dx_1$. Within a plane strain assumption, the displacements are embedded into 3-d by the extension $\mathbf{u}_3 \equiv 0$ and all material computations are performed in 3-d.

First, we study the nonlinear convergence behavior for a single time step (Table 5). We observe that the standard projection method converges quadratically in the final iterations but the iteration starts quite slow since global convergence requires strong damping. The SQP method also shows quadratic convergence but here the global convergence properties are better. Again, the generalized Newton method for the linearized projection method in every SQP step converges quadratically in the final iterations, and again global convergence for the quadratic sub-problems requires strong damping but less damping than the full projection method. Of course, the nonlinear problems in the substeps do not need to be solved exactly.

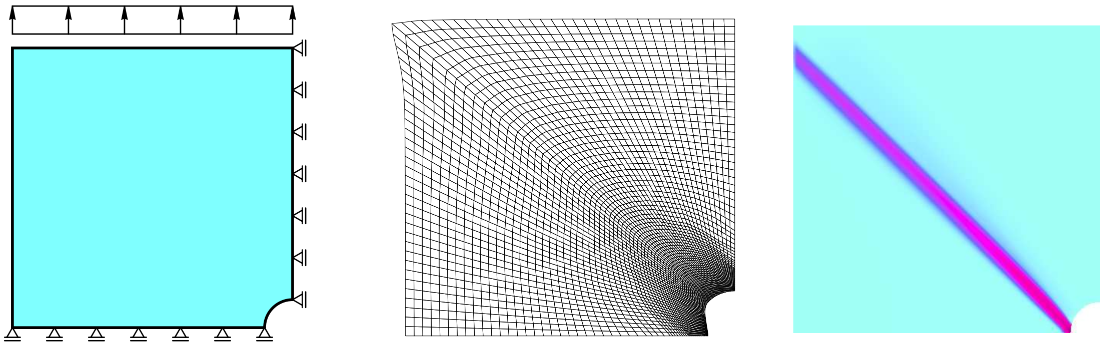

Figure 3: Geometric configuration and boundary conditions (left), deformed configuration for $t = 4.7$ (center), and distribution of the equivalent plastic strain (right) for the benchmark problem.

In an inexact SQP variant, the accuracy requirements for the linearized projection steps can be reduced without affecting the overall SQP convergence.

The next Table (Table 6) studies the dependence on the discretization level. In all cases, the generalized Newton methods for the nonlinear variational problems (23) and (31) are globally convergent (provided a suitable damping strategy is applied) but the number of required steps to obtain a prescribed accuracy is increasing with the number of unknowns. Locally, we observe quadratic convergence close to the solution. This is the expected behavior if the active set of the convex pointwise constraint is (more or less) identified. Altogether, this numerical experiment reflects the fact that the primal displacement approximation in H^1 is not well-posed: stable a priori estimates are available only in the space of bounded deformations, resulting in mesh-dependent discrete estimates [**12**].

On the other hand, the SQP method (and its inexact variant) shows mesh-independent quadratic convergence. Although no formal proof is given for this observation, this is the expected behavior since the the dual stress approximation in L_2 is well-posed and therefore mesh-independent a priori bounds are available.

Projection method			SQP method			inexact SQP method		
(FR)	(CC)	(EE)	(FR)	(CC)	(EE)	(FR)	(CC)	(EE)
ε	ε	24.76562	115.12502	5.093109	ε	115.11406	5.093016	0.144698
ε	ε	17.87826	43.03050	0.797243	ε	43.02698	0.797055	0.048011
ε	ε	13.17991	0.78454	0.074983	ε	0.78515	0.074975	0.022294
ε	ε	9.66825	0.00294	0.000073	ε	0.00293	0.000072	0.000012
ε	ε	6.38058	ε	ε	ε	ε	ε	ε
ε	ε	4.38372						
ε	ε	3.32549						
ε	ε	0.66842						
ε	ε	0.00188						
ε	ε	ε						

$t_n = 4.6$, $\Delta t_n = 0.3$
$\varepsilon < 10^{-10}$
16384 quadrilateral cells, bilinear finite elements

Table 5: Comparison of the convergence behavior of the projection method, the SQP method, and an inexact version of the SQP method for one time step. For the numerical test, the defect of the equations (15a), (15b), (15c) in the Euklidian norm is reduced to $\varepsilon < 10^{-10}$. Note that this is far more accurate than the discretization error of the finite element approximation.

cells	dof	Projection method	SQP method	inexact SQP method
4096	8450	9 Newton steps	5 SQP steps (18 substeps)	5 SQP steps (10 sub.)
16384	33282	10 Newton steps	5 SQP steps (21 substeps)	5 SQP steps (14 sub.)
65536	132098	17 Newton steps	5 SQP steps (23 substeps)	5 SQP steps (16 sub.)
262144	526338	31 Newton steps	5 SQP steps (31 substeps)	5 SQP steps (22 sub.)
1048576	2101250	56 Newton steps	5 SQP steps (42 substeps)	5 SQP steps (31 sub.)

Table 6: Iteration count depending on the discretization level for the projection method, the SQP method, and an inexact version of the SQP method for one time step at $t_n = 4.6$ and $\Delta t_n = 0.3$. The number of substeps counts the number of generalized Newton steps for all SQP steps. Since the numerical expense is dominated by the linear solver within the generalized Newton step, the overall computing time is proportional to the number of Newton steps or total number of substeps in the SQP iteration, respectively.

Conclusion. Although convex programming provides a better understanding of computational plasticity, in many applications there is no need for new solution methods; the well-established projection method is often superior to other methods. On the other hand, this method is not stable, and close to the limit load (even for regularized models with small regularization parameters) the method may deteriorate.

The major advantage of SQP methods is the large flexibility (e. g., using augmented Lagrangians) which allows to enhance and stabilize the method to far more general (and even nonconvex) plasticity models, in particular to multi-yield plasticity or finite plasticity, where the realization of the projection method is not straight-forward. This will be studied in future work.

References

[1] J. Alberty, C. Carstensen, and D. Zarrabi, *Adaptive numerical analysis in primal elastoplasticity with hardening*, Comput. Meth. Appl. Mech. Engrg., 171 (1999), pp. 175–204.

[2] W. Alt, *Nichtlineare Optimierung*, Vieweg, 2002.

[3] P. W. Christensen, *A nonschmooth Newton method for elastoplastic problems*, Comput. Meth. Appl. Mech. Engrg., 191 (2002), pp. 1189–2119.

[4] F. H. Clarke, *Optimization and Nonsmooth Analysis*, Wiley, 1983.

[5] W. Han and B. D. Reddy, *Plasticity: Mathematical Theory and Numerical Analysis*, Springer-Verlag, 1999.

[6] M. Hintermüller, K. Ito, and K. Kunisch, *The primal-dual active set strategy as a semi-smooth Newton method*, SIAM J. Optimization, 13 (2003), pp. 865–888.

[7] M. Hintermüller and M. Ulbrich, *A mesh-independence result for semi-smooth Newton methods*, Mathematical Programming, 101 (2004), pp. 151–184.

[8] R. Klatte and B. Kummer, *Nonsmooth Equations in Optimization*, vol. 60 of Nonconvex Optimization and Its Applications, Kluwer, 1993.

[9] S. Lang, C. Wieners, and G. Wittum, *The application of adaptive parallel multigrid methods to problems in nonlinear solid mechanics*, in Error-Controlled Adaptive Finite Element Methods in Solid Mechanics, E. Stein, ed., New-York, 2002, Wiley, pp. 347–384.

[10] D. Luenberger, *Linear and Nonlinear Programming*, Addison-Wesley, 1984.

[11] J. Nečas, *Introduction to the Theory of Nonlinear Elliptic Equations*, vol. 52 of Teubner-Texte zur Mathematik, Teubner, Leipzig, 1983.

[12] M. Plum and C. Wieners, *Numerical enclosures for variational inequalities*, (2005). submitted.

[13] J. C. Simo and T. J. R. Hughes, *Computational Inelasticity*, Springer-Verlag, 1998.

[14] P. Spellucci, *Numerische Verfahren der nichtlinearen Optimierung*, Birkhäuser, 1993.

[15] R. Temam, *Mathematical Problems in Plasticity*, Bordas, Paris, 1985.

[16] C. Wieners, *Distributed point objects. A new concept for parallel finite elements*, in Domain Decomposition Methods in Science and Engineering, R. Kornhuber, R. Hoppe, J. Périaux, O. Pironneau, O. Widlund, and J. Xu, eds., vol. 40 of Lecture Notes in Computational Science and Engineering, Springer, 2004, pp. 175–183.

Fakultät für Mathematik, Universität Karlsruhe, Kaiserstr. 12, 76128 Karlsruhe, Germany.

E-mail address: wieners@math.uni-karlsruhe.de

IWRMM-Preprints seit 2004

Nr. 04/01	Andreas Rieder: Inexact Newton Regularization Using Conjugate Gradients as Inner IteractionMichael
Nr. 04/02	Jan Mayer: The ILUCP preconditioner
Nr. 04/03	Andreas Rieder: Runge-Kutta Integrators Yield Optimal Regularization Schemes
Nr. 04/04	Vincent Heuveline: Adaptive Finite Elements for the Steady Free Fall of a Body in a Newtonian Fluid
Nr. 05/01	Götz Alefeld, Zhengyu Wang: Verification of Solutions for Almost Linear Complementarity Problems
Nr. 05/02	Vincent Heuveline, Friedhelm Schieweck: Constrained H^1-interpolation on quadrilateral and hexahedral meshes with hanging nodes
Nr. 05/03	Michael Plum, Christian Wieners: Enclosures for variational inequalities
Nr. 05/04	Jan Mayer: ILUCDP: A Crout ILU Preconditioner with Pivoting and Row Permutation
Nr. 05/05	Reinhard Kirchner, Ulrich Kulisch: Hardware Support for Interval Arithmetic
Nr. 05/06	Jan Mayer: ILUCDP: A Multilevel Crout ILU Preconditioner with Pivoting and Row Permutation
Nr. 06/01	Willy Dörfler, Vincent Heuveline: Convergence of an adaptive *hp* finite element strategy in one dimension
Nr. 06/02	Vincent Heuveline, Hoang Nam-Dung: On two Numerical Approaches for the Boundary Control Stabilization of Semi-linear Parabolic Systems: A Comparison
Nr. 06/03	Andreas Rieder, Armin Lechleiter: Newton Regularizations for Impedance Tomography: A Numerical Study
Nr. 06/04	Götz Alefeld, Xiaojun Chen: A Regularized Projection Method for Complementarity Problems with Non-Lipschitzian Functions
Nr. 06/05	Ulrich Kulisch: Letters to the IEEE Computer Arithmetic Standards Revision Group
Nr. 06/06	Frank Strauss, Vincent Heuveline, Ben Schweizer: Existence and approximation results for shape optimization problems in rotordynamics
Nr. 06/07	Kai Sandfort, Joachim Ohser: Labeling of n-dimensional images with choosable adjacency of the pixels
Nr. 06/08	Jan Mayer: Symmetric Permutations for I-matrices to Delay and Avoid Small Pivots During Factorization
Nr. 06/09	Andreas Rieder, Arne Schneck: Optimality of the fully discrete filtered Backprojection Algorithm for Tomographic Inversion
Nr. 06/10	Patrizio Neff, Krzysztof Chelminski, Wolfgang Müller, Christian Wieners: A numerical solution method for an infinitesimal elasto-plastic Cosserat model
Nr. 06/11	Christian Wieners: Nonlinear solution methods for infinitesimal perfect plasticity

Eine aktuelle Liste aller IWRMM-Preprints finden Sie auf:

www.mathematik.uni-karlsruhe.de/iwrmm/seite/preprints